REVIEW ARTICLE

What the structure of a calcium pump tells us about its mechanism

Anthony G. LEE[1] and J. Malcolm EAST

Division of Biochemistry and Molecular Biology, School of Biological Sciences, University of Southampton, Southampton SO16 7PX, U.K.

The report of the crystal structure of the Ca^{2+}-ATPase of skeletal muscle sarcoplasmic reticulum in its Ca^{2+}-bound form [Toyoshima, Nakasako and Ogawa (2000) Nature (London) **405**, 647–655] provides an opportunity to interpret much kinetic and mutagenic data on the ATPase in structural terms. There are no large channels leading from the cytoplasmic surface to the pair of high-affinity Ca^{2+} binding sites within the transmembrane region. One possible access pathway involves the charged residues in transmembrane α-helix M1, with a Ca^{2+} ion passing through the first site to reach the second site. The Ca^{2+}-ATPase also contains a pair of binding sites for Ca^{2+} that are exposed to the lumen. In the four-site model for transport, phosphorylation of the ATPase leads to transfer of the two bound Ca^{2+} ions from the cytoplasmic to the lumenal pair of sites. In the alternating four-site model for transport, phosphorylation leads to release of the bound Ca^{2+} ions directly from the cytoplasmic pair of sites, linked to closure of the pair of lumenal binding sites. The lumenal pair of sites could involve a cluster of conserved acidic residues in the loop between M1 and M2. Since there is no obvious pathway from the high-affinity sites to the lumenal surface of the membrane, transport of Ca^{2+} ions must involve a significant change in the packing of the transmembrane α-helices. The link between the phosphorylation domain and the pair of high-affinity Ca^{2+} binding sites is probably provided by two small helices, P1 and P2, in the phosphorylation domain, which contact the loop between transmembrane α-helices M6 and M7.

Key words: Ca^{2+}-ATPase, Ca^{2+} transport, membrane proteins, sarcoplasmic reticulum, skeletal muscle.

INTRODUCTION

The P-type ATPases are a large family of membrane proteins that are responsible for the active transport of cations across biological membranes. The family can be divided into three major groups: those that transport heavy metals such as Cu^{2+}, Cd^{2+} and Hg^{2+}, the plant and fungal H^+-ATPases, and the (Na^+,K^+)- and Ca^{2+}-ATPases [1,2]. The energy required to move cations against their electrochemical potential gradients comes from the hydrolysis of the terminal phosphate bond of ATP, to give ADP and P_i. During the process, an Asp residue in an invariant sequence DKTGT(I/L)T on the ATPase becomes phosphorylated; it is this feature that distinguishes the P-type ATPases from other transport ATPases, such as the V-type ATPases and the F_0F_1-ATPases.

The Ca^{2+}-ATPase of muscle sarcoplasmic reticulum (SR) or endoplasmic reticulum (ER) consists of a single polypeptide chain, unlike other ATPases, which exist as α,β-heterodimers. Three genes code for the SR/ER Ca^{2+}-ATPases (SERCAs): *SERCA1*, *SERCA2* and *SERCA3*. The *SERCA1* gene encodes the Ca^{2+}-ATPase of the SR, which is expressed mainly in fast-twitch skeletal muscle. The recent publication of the X-ray crystal structure of the SERCA1 Ca^{2+}-ATPase of rabbit skeletal muscle SR by Toyoshima et al. [3] provides many insights into the mechanism of the Ca^{2+}-ATPase. The aim of this review is to describe the mechanism of the Ca^{2+}-ATPase, and to show how far the mechanism can be interpreted in terms of the high-resolution crystal structure.

OVERALL STRUCTURE OF THE Ca^{2+}-ATPase

Sequencing of the Ca^{2+}-ATPase led to a predicted secondary structure comprising three globular cytoplasmic domains connected by a helical stalk segment, S, to ten transmembrane α-helices (M1–M10) [4], as shown in modified form in Figure 1. The first of the cytoplasmic domains, initially referred to as the transduction or β-strand domain, is a 125-residue loop connected to stalk regions S2 and S3. A larger loop of about 410 residues, connected to stalks S4 and S5, was originally proposed to consist of a phosphorylation domain (P domain) (containing the residue Asp-351 that becomes phosphorylated), followed by a nucleotide binding domain (N domain) and a hinge region connecting to S5. This original domain assignment was modified following the realization that the Ca^{2+}-ATPase belongs to a superfamily of haloacid dehalogenases (HADs) that includes, as well as the P domain of the P-type ATPases, the catalytic domains of HADs, phosphoglycomutases and serine/threonine phosphatases, all of which form an aspartyl ester intermediate [5,6]. The crystal structure of L-2 HAD from *Pseudomonas* sp. YL (1JUD) shows a catalytic domain consisting of a typical Rossman fold of a six-stranded β-sheet surrounded by five α-helices, with a subdomain inserted into the catalytic domain between the first β-sheet and the first α-helix of the catalytic domain [7]. By analogy, it was therefore suggested that the N domain of the Ca^{2+}-ATPase formed an insert within a combined phosphorylation/hinge domain, as shown in Figure 1 [6]. These predictions are largely in agreement with the X-ray structure for the Ca^{2+}-ATPase (Figure 2).

The crystal structure of the Ca^{2+}-ATPase shows the presence of ten transmembrane α-helices, with three clear globular domains on the cytoplasmic side of the membrane with small loops on the lumenal side (Figure 2). The number of transmembrane α-helices has been the subject of some controversy. Secondary structure predictions all agreed that four transmembrane α-helices were present in the N-terminal half of the protein, but

Abbreviations used: A domain, activation domain; N domain, nucleotide binding domain; P domain, phosphorylation domain; ER, endoplasmic reticulum; SR, sarcoplasmic reticulum; SERCA, sarcoplasmic reticulum/endoplasmic reticulum Ca^{2+}-ATPase; HAD, haloacid dehalogenase; $C_{12}E_8$, octa(ethylene glycol) monododecyl ether; TNP-AMP, 2′,3′-*O*-(2,4,6-trinitrophenyl)-AMP; PC, phosphatidylcholine.

[1] To whom correspondence should be addressed (e-mail agl@soton.ac.uk).

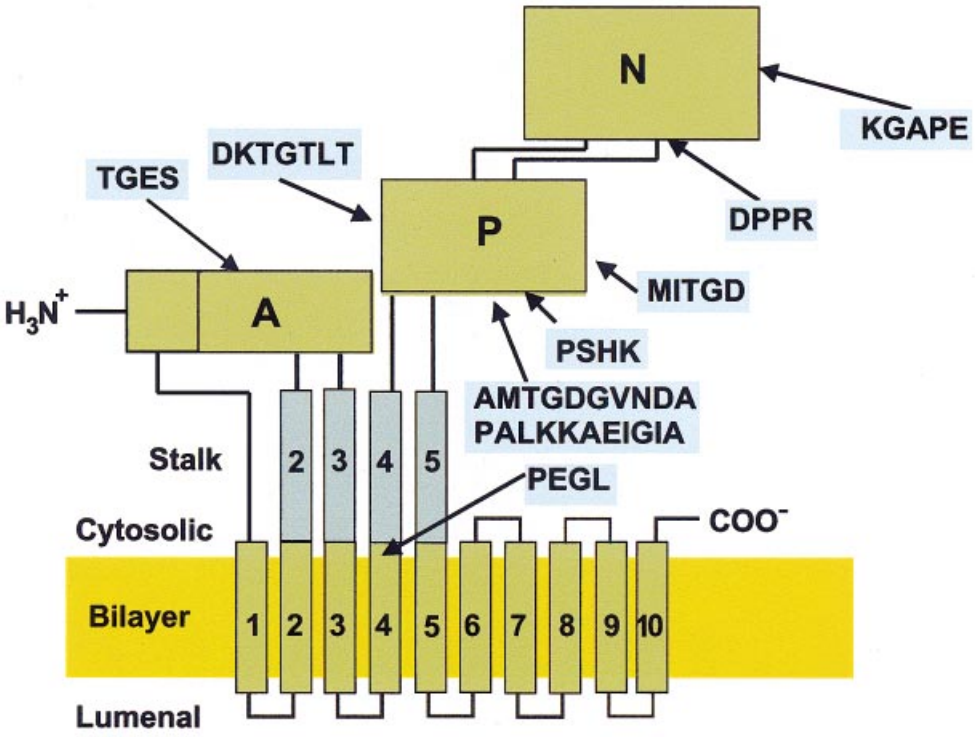

Figure 1 Secondary structure of the Ca^{2+}-ATPase based on the crystal structure of Toyoshima et al. [3]

The three cytoplasmic domains A (activation), P (phosphorylation) and N (nucleotide binding) are connected to the ten transmembrane α-helices by four α-helical stalks (numbered 2–5, in accordance with the transmembrane α-helix to which they are attached). The N domain forms an insert into the P domain. The locations of a number of conserved motifs are shown.

disagreed with regard to the number present in the C-terminal half. Confirmation of the localization of the N- and C-termini of the Ca^{2+}-ATPase on the cytoplasmic side by antibody binding studies showed that the number of transmembrane α-helices had to be even [8]. A model with ten transmembrane α-helices was supported by antibody binding studies, which showed that residues between Lys-870 and Ile-890 (the M7–M8 loop) were on the lumenal side of the membrane [9,10].

Whereas secondary structure predictions suggested the presence of five α-helices in the stalk region connecting the cytoplasmic domains to the transmembrane region [4], in fact there are only four, connected to transmembrane α-helices M2–M5; N-terminal residues 1–50 are connected directly to M1 without the predicted stalk region S1. The stalk regions consist of extensions of the transmembrane α-helices above the expected membrane surface. The stalk regions of the α-helices differ from the transmembrane regions in being much less hydrophobic and in containing a high proportion of charged residues, particularly Glu and Asp. The stalk S5 is particularly remarkable, forming, with the transmembrane α-helix M5, a continuous 41-residue α-helix stretching from Phe-740 to Ala-780, giving the appearance of a pillar running up the centre of the protein.

At the centre of the cytoplasmic headpiece is the P domain. The P domain is made up of two parts, widely separated in the amino acid sequence: an N-terminal region from about Asn-330 to Asn-359 and a larger C-terminal region from Lys-605 to Asp-737. The structure of the P domain is analogous with that of the HADs, as predicted by the sequence identity [6]. The N domain is the largest of the three cytoplasmic domains, running roughly from Gln-360 to Arg-604. The N domain is inserted into the sequence between the two components making up the P domain, like the subdomain inserted into the catalytic domain of the HADs. The N domain is a seven-stranded antiparallel β-sheet sandwiched by two bundles of α-helices linked to the P domain by two loops. This presumably gives the N domain considerable flexibility with respect to the rest of the structure, and explains the fact that several proteases release a stable fragment of the Ca^{2+}-ATPase, comprising residues Thr-357 to Thr-608, which retains the ability to bind nucleotides [11].

The 145 residues between stalks S2 and S3, together with the 50 residues in the N-terminal region, form what has been called the activation domain (A domain) by Toyoshima et al. [3]; this was previously called the transduction or β-strand domain. The region between S2 and S3 forms a distorted jelly-roll structure, and the N-terminal region contains two short helices [3]. The domain is almost isolated from the rest of the structure, being connected to the transmembrane region by three long loops. The second trypsin cleavage site (T2) at Arg-198 is in an exposed loop on the outermost edge of the A domain. Trypsin cleavage at T2 is enhanced by binding of Ca^{2+} and blocked by phosphorylation [12], suggesting that this domain might move during transport. The N-terminal region shows little identity with the other P-type ATPases. Daiho et al. [13] found that deletion or substitution of some of the residues in the Ala-3 to Thr-9 region led to a much reduced level of expression, suggesting that the N-terminal region is critical for correct folding of the ATPase.

The transmembrane region consists of ten transmembrane α-helices. Two Ca^{2+} ions are bound in the transmembrane region between helices M4, M5, M6 and M8 (Figure 2). Ca^{2+} ions bound to proteins are typically co-ordinated by seven oxygen

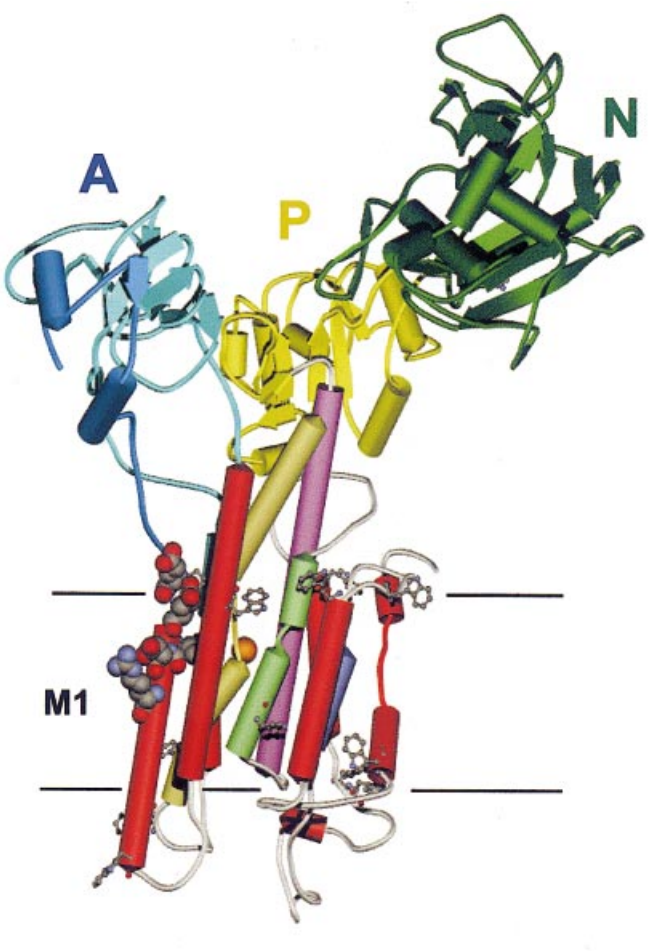

Figure 2 Structure of the Ca^{2+}-ATPase

The three cytoplasmic domains A, P and N are coloured blue, yellow and green respectively. The N-terminal region is coloured dark blue. The four transmembrane α-helices involved in binding Ca^{2+} at the high-affinity pair of sites are coloured as follows: M4, yellow; M5, lilac; M6, green; M8, blue; the other transmembrane α-helices are coloured red. Of the two bound Ca^{2+} ions (orange), only one is visible in this view. Trp residues are shown in ball-and-stick representation. Charged residues in helix M1 are shown in space-fill representation. (PDB file 1EUL).

ligands, in a non-symmetrical arrangement [14], and that is what is seen here (Figure 3). The two Ca^{2+} ions are bound side by side, 5.7 Å apart, at almost the same distance from the membrane surface. Site I contains oxygen ligands from M5, M6 and M8, whereas site II contains oxygen ligands predominantly from M4. The two sites are bridged by Asp-800 in M6, which contributes a carboxyl oxygen to both sites. Co-ordination at site I is provided by side-chain oxygens of Asn-768 and Glu-771 from M5, Thr-799 and Asp-800 from M6, and Glu-908 from M8. Disruption of the helical structure of M6 around Asp-800 and Gly-801 is required to allow both Thr-799 and Asp-800 to contribute to the site [3]. The oxygen atoms are arranged roughly in a plane, except for the two carboxyl oxygens of Glu-771, which are located beneath (on the lumenal side of) the plane. Site II is markedly different, with a much more uniform distribution of oxygen ligands around the Ca^{2+} ion and with contributions from both side-chain and backbone oxygens. Oxygens are provided by side-chain oxygens of Asn-796 and Asp-800 from M6 and Glu-309 from M4, and by backbone oxygens of Val-304, Ala-305 and Ile-307 from M4. Again, this pattern of co-ordination requires that the helix that contributes most ligands to the site (M4) is unwound between Ile-307 and Gly-310. The unwound region of M4 contains the PEGL (Pro-Glu-Gly-Leu) motif found in the P-type ATPases; the Glu residue is replaced by Cys or His in ATPases that transport heavy metals [2].

The two sites are linked most obviously by Asp-800, which co-ordinates both Ca^{2+} ions, and also by a hydrogen bond between Asn-768 at site I and Ala-306 in the Val-304–Glu-309 loop important in co-ordinating Ca^{2+} at site II. Extensive hydrogen-bonding networks link the residues at both sites to residues in neighbouring helices. This is obviously important in stabilizing the unwound helices within the environment of the lipid bilayer, since the energetic cost of losing a hydrogen bond in a hydrophobic environment is very high [15].

MECHANISM OF THE Ca^{2+}-ATPase

The mechanism of the Ca^{2+}-ATPase is usually discussed in terms of the E1–E2 model developed from the Post-Albers scheme for (Na^+,K^+)-ATPase, as shown in Scheme 1 [16]. The model proposes that the Ca^{2+}-ATPase can exist in one of two distinct forms, E1 and E2. In its original form, the model further proposed that, in the E1 conformation, the ATPase contained two high-affinity binding sites for Ca^{2+} that were exposed to the cytoplasm, whereas in the E2 conformation these two sites had been transformed into low-affinity sites exposed to the lumen of the SR; this is the alternating-site model (Figure 4). Following the binding of MgATP to the Ca^{2+}-bound form of the ATPase, the ATPase is phosphorylated and undergoes a change in conformation to $E2PCa_2$, a state in which the two Ca^{2+} binding sites are of low affinity and inwardly facing. Following loss of Ca^{2+} to the lumen of the SR, the ATPase is dephosphorylated and is recycled to E1.

The phosphorylation events on the Ca^{2+}-ATPase are reversible. The phosphorylated ATPase can react with ADP in the presence of Ca^{2+} to regenerate ATP. More surprisingly, the dephosphorylation event is also reversible, so that incubation of the Ca^{2+}-ATPase with P_i in the absence of cytoplasmic Ca^{2+} leads to phosphorylation of the ATPase [17–20]. Since acyl phosphates have larger negative free energies of hydrolysis than even ATP [16], spontaneous formation of an acyl phosphate, in the absence of any source of energy, is unusual. It implies stabilization of the acyl phosphate on the ATPase, presumably by interaction with Mg^{2+} (necessary for the reaction) and with groups on the ATPase. In this back-reaction (Scheme 2), Mg^{2+} and P_i bind randomly to the ATPase. The level of phosphorylation decreases markedly with increasing pH, since although $H_2PO_4^-$ and HPO_4^{2-} can both bind to the ATPase, only binding of $H_2PO_4^-$ leads to phosphorylation, with an equilibrium constant (K_5 in Scheme 2) of 2.3 [21].

Many the features of this reaction scheme are still controversial. As a minimum, we can say that binding of Ca^{2+} to the high-affinity sites on the ATPase causes a change in chemical reactivity, from being reactive with P_i and water in the absence of Ca^{2+} to being reactive with ATP and ADP in the presence of Ca^{2+} [22]. A wide range of experiments on the rate of phosphorylation of the ATPase by ATP can be interpreted simply in these terms, without the need for two conformations (E1 and E2) for the ATPase [23,24]. However, a variety of spectroscopic experiments have been interpreted in terms of a pH-dependent equilibrium between two forms, E1 and E2 (see [25]). The equilibrium between E1 and E2 fits the simple scheme shown in Scheme 3, with a value of K_1 of 4 with stronger binding of H^+ to E2 ($K_3 = 3 \times 10^8\ M^{-1}$) than to E1 ($K_2 = 5 \times 10^5\ M^{-1}$) explaining the shift towards E2 with decreasing pH [25].

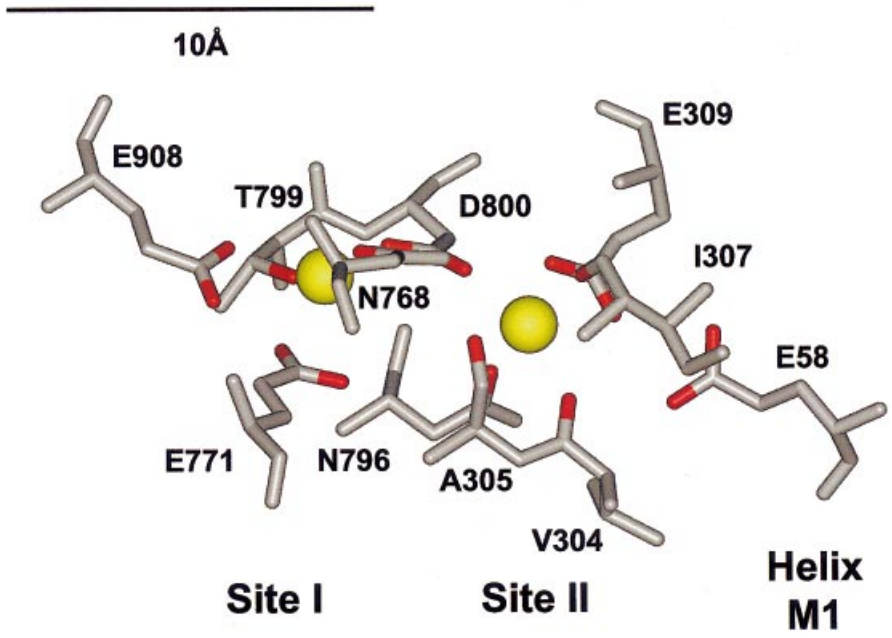

Figure 3 Two high-affinity Ca^{2+} binding sites on the Ca^{2+}-ATPase

Residues contributing to the binding sites are shown. Also shown is Glu-58 on transmembrane α-helix M1.

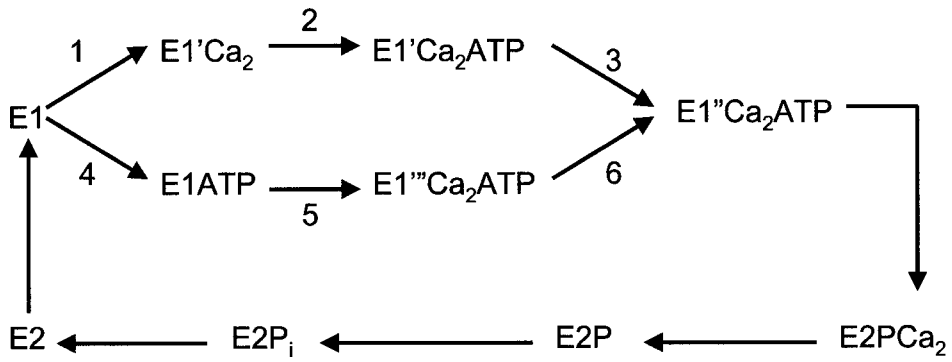

Scheme 1 E1/E2 scheme for the Ca^{2+}-ATPase

Either ATP or Ca^{2+} can bind first to the E1 conformation of the Ca^{2+}-ATPase. A series of conformational changes leads to the intermediate E1″Ca_2·ATP, which undergoes phosphorylation to give E2PCa_2. This loses Ca^{2+} into the lumen and can then be dephosphorylated to form E2, which can return to E1.

More recently, it has become clear that the alternating-site model shown in Figure 4 is not compatible with much of the kinetic and equilibrium data available for the Ca^{2+}-ATPase. In particular, the alternating-site model predicts that binding of Ca^{2+} to the ATPase from the lumenal side (to the E2 conformation) will be competitive with binding of Ca^{2+} from the cytoplasmic side (to the E1 conformation). In fact, it has been shown that the presence of Ca^{2+} in the lumen of the SR has no effect on the affinity of the cytoplasmic sites for Ca^{2+}, or on the proportions of the ATPase present in the E1 and E2 conformations at equilibrium [20,21]. A possible explanation for these results might have been that Ca^{2+} is unable to bind to the E2 conformation from the lumenal side of the membrane, although it must be able to bind to E2P, since E2PCa_2 is an intermediate in the reaction cycle. However, this suggestion would be inconsistent with the observed effects of lumenal Ca^{2+} on the level of phosphorylation of the ATPase by P_i. If lumenal Ca^{2+} could bind only to E2P, and not to E2, the presence of very high concentrations of lumenal Ca^{2+} would pull the equilibrium for phosphorylation of the ATPase by P_i fully over to the phosphorylated form (Scheme 4), and this is not seen [17,20]. Rather, only a proportion of the ATPase becomes phosphorylated, depending on the concentrations of Mg^{2+} and P_i. This means that the unphosphorylated and phosphorylated forms of the ATPase must bind an equal number of Ca^{2+} ions from the lumenal side. Thus lumenal Ca^{2+} must be able to bind to both E2 and E2P, and yet not compete with binding of Ca^{2+} to the cytoplasmic pair of sites. The simplest explanation is that the Ca^{2+}-ATPase contains separate pairs of cytoplasmic and lumenal binding sites for Ca^{2+}, so that Ca^{2+} can bind simultaneously from the two sides of the membrane [20]; this is the four-site model shown in Figure 4. In terms of this four-site model, the E1 and E2 conformations differ

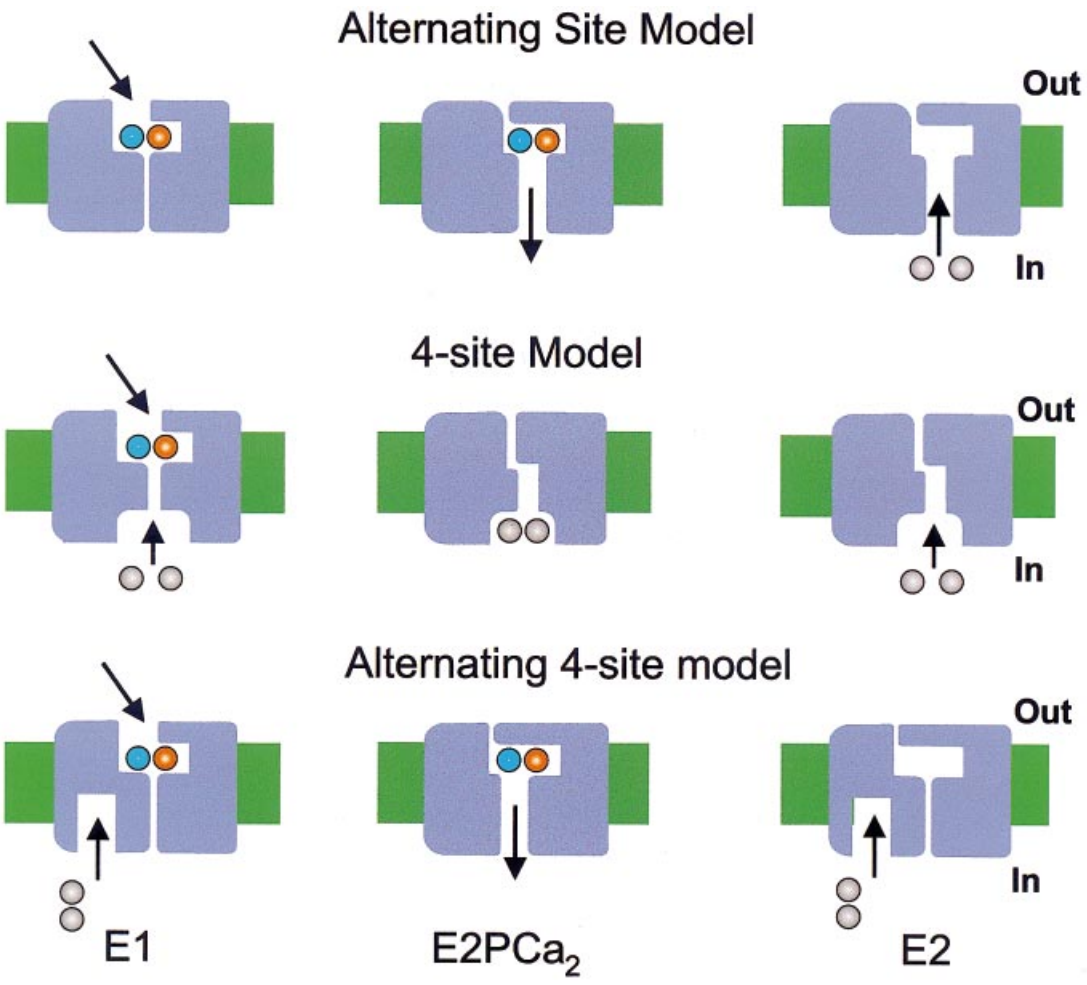

Figure 4 Three models for transport of Ca^{2+} by the Ca^{2+}-ATPase

The alternating-site model proposes the presence of one pair of sites which alternate from being exposed to the cytoplasm in the E1 conformation to being exposed to the lumen in the E2 and $E2PCa_2$ states. In the four-site model, two Ca^{2+} ions move on phosphorylation of the Ca^{2+}-ATPase from a pair of sites exposed to the cytoplasm in E1 to a separate pair of sites exposed to the lumen in $E2PCa_2$ and E2. In the alternating four-site model, the pair of transport sites changes from being exposed to the cytoplasm in E1 to being exposed to the lumen in $E2PCa_2$; in the E2 conformation, the transport sites are not accessible from either side of the membrane. Phosphorylation also leads to closure of a pair of lumenal sites. The net result is that only two Ca^{2+} ions can bind to all E2 conformations from the lumenal side of the membrane. The importance of the lumenal pair of sites in the alternating four-site model is to prevent the build-up of large amounts of phosphorylated ATPase as a result of back-reaction with P_i in the cytoplasm. In all three models, binding of Ca^{2+} to the cytoplasmic sites is ordered; binding of the second Ca^{2+} ion (blue) blocks release of the first Ca^{2+} ion (orange). Lumenal Ca^{2+} ions are shown in grey.

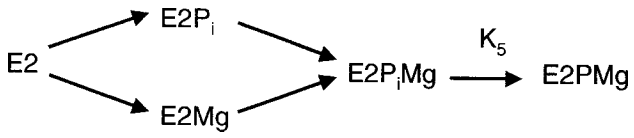

Scheme 2 Phosphorylation by P_i

in that, whereas in the E1 conformation the Ca^{2+}-ATPase can bind a total of four Ca^{2+} ions, in the E2 conformation the pair of cytoplasmic sites are unavailable for binding and Ca^{2+} can only bind to the lumenal pair of sites. In the four-site model, phosphorylation of $E1Ca_2$ to give $E2PCa_2$ causes the cytoplasmic pair of sites to close as the pair of Ca^{2+} ions transfer to the lumenal pair of sites, from which they are released into the lumen of the SR [20].

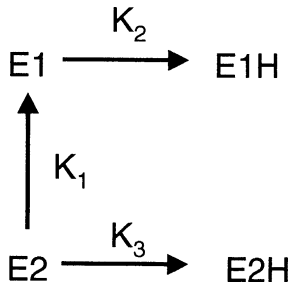

Scheme 3 Effect of pH on the E1/E2 equilibrium

A major difference between the alternating- and four-site models for transport is, therefore, that in the alternating-site model the two bound Ca^{2+} ions are released directly to the

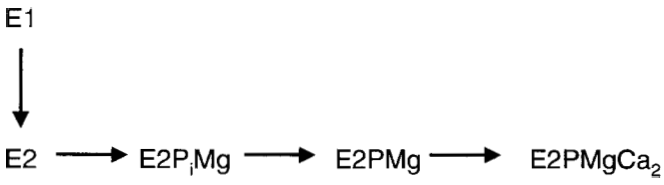

Scheme 4 Effect of lumenal Ca^{2+} on phosphorylation by P_i

lumen from the pair of sites to which they first bind (the cytoplasmic pair of sites), whereas in the four-site model the two Ca^{2+} ions are released from the other, lumenal pair of sites. However, as will be described later, experiments using site-directed mutagenesis support a model in which the bound Ca^{2+} ions are released directly into the lumen from the cytoplasmic pair of sites. This is consistent with a different formulation of the four-site model, which we have called the alternating four-site model (Figure 4). This proposes that phosphorylation of the ATPase results in a change in the cytoplasmic pair of binding sites into a state in which they are exposed to the lumen and of low affinity for Ca^{2+}, as in the alternating-site model. Phosphorylation also results in closing of the pair of lumenal binding sites on the ATPase. Finally, the pair of transport sites are unavailable for binding Ca^{2+} from either side of the membrane in the E2 state (Figure 4). This ensures that E2 and the phosphorylated ATPase (E2P) can both bind only two Ca^{2+} ions from the lumenal side, as required by the P_i phosphorylation experiments. The importance of the lumenal pair of sites in the alternating four-site model would be to prevent the build-up of large amounts of phosphorylated ATPase as a result of back-reaction with P_i in the cytoplasm; in the absence of such a pair of lumenal sites, binding of lumenal Ca^{2+} to E2P would highly favour the phosphorylated form, as already explained. The differences between these two models will be explored further later in this review.

Binding of Ca^{2+} to the high-affinity pair of sites on E1 is co-operative, probably with a conformation change occurring between the binding of the first and second Ca^{2+} ions, according to the scheme:

$$E1 + Ca^{2+} \leftrightarrow E1Ca \leftrightarrow E1'Ca + Ca^{2+} \leftrightarrow E1'Ca_2$$

where the E1 conformation possesses only a single high-affinity Ca^{2+} binding site, and the conformation change $E1Ca \rightarrow E1'Ca$ is necessary to create the second site [25,26].

The substrate for the ATPase reaction is MgATP, but Mg^{2+} and ATP can bind and dissociate from the catalytic site independently or as the MgATP complex [27]. Mg^{2+} can bind to preformed $E1'Ca_2 \cdot ATP$, so that the catalytic Mg^{2+} binding site cannot be 'buried' underneath the ATP. Similarly, since Mg^{2+} can dissociate from the catalytic site independently of ATP, the phosphates of ATP cannot be held in a pocket by the Mg^{2+} ion, since in such a model the Mg^{2+} ion would have to dissociate from the ATPase before ATP could dissociate [27]. This mirrors the observation that binding of Mg^{2+} and P_i are random in the back-phosphorylation reaction, as shown in Scheme 2.

The ATPase can either first bind Ca^{2+} and then MgATP, or first bind MgATP and then Ca^{2+}; the differences between these two pathways are described in more detail below. Taking just the upper pathway in Scheme 1 as an example, when MgATP is added to preformed $E1'Ca_2$, the rate-determining step for phosphorylation is a conformational change following the binding of MgATP ($E1'Ca_2 \cdot ATP \rightarrow E1''Ca_2 \cdot ATP$ step in Scheme 1); this is followed by fast phosphorylation with a rate constant (k) of $\geqslant 1000\ s^{-1}$ [28]. The conformational change is thought to involve movement of the γ-phosphate of ATP towards the phosphorylation site, aligning it for rapid phosphoryl transfer [28].

Only a single Ca^{2+}-bound phosphorylated form ($E2PCa_2$) is shown in Scheme 1. In the original formulation of the E1–E2 model, two phosphorylated forms, $E1PCa_2$ and $E2PCa_2$, were included, giving the pathway $E1''Ca_2 \cdot ATP \rightarrow E1PCa_2 \rightarrow E2PCa_2$ [16]. The evidence for two forms came from experiments in which ADP was added to the ATPase phosphorylated with ATP in the presence of Ca^{2+}. A biphasic loss of phosphoenzyme was observed, and it was proposed that the component reacting rapidly with ADP was $E1PCa_2$ (reacting with ADP to give ATP) and that the slowly reacting component was $E2PCa_2$, which had to undergo the $E2PCa_2 \rightarrow E1PCa_2$ (slow) transition before reaction was possible with ADP [16]. In this scheme, the relative proportions of the fast- and slow-reacting components depend on the ratio of $E1PCa_2$ to $E2PCa_2$ at steady state, and is independent of the ADP concentration added. However, Pickart and Jencks [29] found that the proportions of the two components did depend on the ADP concentration; they showed that the decay was, in fact, consistent with the rapid formation of enzyme-bound ATP, followed by a slow dissociation of the bound ATP:

$$E2PCa_2 + ADP \leftrightarrow E2PCa_2 \cdot ADP \leftrightarrow E1''Ca_2 \cdot ATP \leftrightarrow E1'Ca_2 + ATP$$

This model predicts that the magnitude of the fast component (the burst size), α, is dependent on the concentration of ADP, and is given by:

$$\alpha = [1 + K_{int}(1 + K_d^{ADP}/[ADP])]^{-1}$$

and the rate constant k for the slow component is given by:

$$k = \alpha k_{off}$$

where K_d^{ADP} is the dissociation constant for ADP, K_{int} is the equilibrium constant for phosphorylation on the ATPase, and k_{off} is the rate constant for the dissociation of ATP. Thus, under conditions where the ATPase is fully Ca^{2+}-bound, the presence of a single form of the ATPase will give biphasic dephosphorylation on addition of ADP. These results do not, therefore, require the existence of two forms of the ATPase, $E1PCa_2$ and $E2PCa_2$. In Scheme 1 the singly phosphorylated, Ca^{2+}-bound form of the ATPase has been designated $E2PCa_2$, according to the definition being used here that the E1 and E2 conformations differ in that E2 conformations cannot bind Ca^{2+} from the cytoplasmic side of the membrane.

The value of K_{int} describing the overall equilibrium $E1'Ca_2 \cdot ATP \leftrightarrow E2PCa_2 \cdot ADP$ is 0.48 [30]. This can be compared with the formation of an acyl phosphate from a carboxylate group and ATP in solution, which is unfavourable, being described by an equilibrium constant of 6×10^{-3} [16,31]. The large increase in equilibrium constant for phosphorylation on the Ca^{2+}-ATPase presumably reflects favourable interactions between the phosphate group and the enzyme in the phosphorylated ATPase, and also a destabilization of ATP when bound to the ATPase, as described later.

MgATP, as well as being the substrate for the ATPase, increases the rates of a number of the steps in the reaction cycle, including the rates of the $E2 \rightarrow E1$ step, of Ca^{2+} binding, of Ca^{2+} release into the lumen and of dephosphorylation, resulting in a complex dependence of overall rate on ATP concentration (see [32]). The observation that MgATP increases the rate of dephosphorylation [33] shows that MgATP must be able to bind to the phosphorylated ATPase; this is also consistent with the observation that MgATP can bind to the ATPase complexed with

vanadate, an analogue of P_i that binds with high affinity to the ATPase [34]. Many of these observations can be explained by assuming that MgATP binds to the nucleotide binding site on the phosphorylated ATPase that is made vacant when ADP dissociates [32]. This does, however, raise a problem. It has been reported that the catalytic Mg^{2+} ion remains bound to the ATPase following phosphorylation [35–37]. Thus binding of MgATP to the phosphorylated ATPase would give a species with two bound Mg^{2+} ions, and there is no direct evidence for such a species. Binding of free ATP to the phosphorylated ATPase would give a species with a single bound Mg^{2+} ion, but the concentration of free ATP present under the normal assay conditions of high Mg^{2+} concentrations would be too low to play any significant role in the reaction [32]. Possibly MgATP binds to the phosphorylated ATPase, forming a transitory complex with two bound Mg^{2+} ions, followed by rapid loss of one of the Mg^{2+} ions. An alternative possibility is that MgATP binds to the phosphorylated ATPase at a site other than the catalytic site; although there is no direct evidence for two nucleotide binding sites on the Ca^{2+}-ATPase, there has been considerable discussion about this possibility.

WHAT THE STRUCTURE TELLS US

Ca^{2+} binding

The structure reported by Toyoshima et al. [3] is for a crystal of the Ca^{2+}-ATPase grown at pH 6.0 in the presence of the detergent octa(ethylene glycol) monododecyl ether ($C_{12}E_8$) and high concentrations of Ca^{2+} [3]. The crystal structure therefore corresponds to the E1′Ca_2 state. The affinity of the ATPase for Ca^{2+} at pH 6.0 is approx. 10 μM [38], so that it is initially surprising that crystallization of the ATPase requires a Ca^{2+} concentration greater than 100 μM [39,40]. However, the detergent $C_{12}E_8$ has complex effects on the properties of the Ca^{2+}-ATPase [41], including a reduction in affinity for Ca^{2+} [42,43], and the presence of $C_{12}E_8$ during crystallization could therefore explain the requirement for a high concentration of Ca^{2+}.

The two Ca^{2+} ions are bound to residues identified previously by mutagenesis. Residues presumed to be at the Ca^{2+} binding sites were identified from mutations that blocked Ca^{2+}-dependent phosphorylation by ATP, but which left Ca^{2+}-independent phosphorylation by P_i unaltered [44]. Glu-309, Glu-771, Asp-800, Glu-908, Asn-796 and Thr-799 were assigned to the Ca^{2+} binding sites in this way (reviewed in [45]). Assignment of residues to each of the two Ca^{2+} binding sites was made on the basis that binding of Ca^{2+} to just the first of the two Ca^{2+} binding sites could block phosphorylation of the ATPase by P_i [46]. Mutation of Glu-309 gave a mutant that was able to bind a single Ca^{2+} ion [47,48], and Ca^{2+} was able to prevent phosphorylation by P_i, suggesting that the first Ca^{2+} ion binding site was intact on the ATPase, and thus that Glu-309 was part of site II [49]. Mutation of Asn-796 also gave a mutant that bound a single Ca^{2+} ion; the double mutation of both Glu-309 and Asn-796 still allowed a single Ca^{2+} ion to bind, showing that Asn-796 and Glu-309 contribute to the same Ca^{2+} ion binding site [48]. In contrast with these mutations, mutation of Glu-771 or Glu-908 reduced the Ca^{2+} affinity measured both by inhibition of phosphorylation by P_i and by stimulation of phosphorylation by ATP, suggesting that these two residues are located at site I. Similar arguments were used to suggest that Thr-799 is at site I, whereas Asn-796 is at site II [50]. Mutation of Asp-800 gave intermediate properties, suggesting that it could contribute to both sites [49].

Further experiments have made use of the non-phosphorylating substrate analogue CrATP, which traps Ca^{2+} bound to the ATPase in an 'occluded' state from which Ca^{2+} is lost very slowly, possibly representing an intermediate state in the normal transport cycle [51]. Whereas mutation of most Ca^{2+} binding residues blocked occlusion of Ca^{2+} on addition by CrATP, mutation of Glu-908 at site I to Ala unexpectedly still allowed Ca^{2+} occlusion; it was therefore suggested that Glu-908 was less important in Ca^{2+} binding than the other acidic residues [50]. Although this suggestion is not borne out by the crystal structure (Figure 3), it does imply that site II is a more important site in 'closing off' the binding sites than site I. An interesting comparison can be made with the plasma membrane Ca^{2+}-ATPase, which binds a single Ca^{2+} ion. The plasma membrane Ca^{2+}-ATPase contains just two of the acidic residues present in transmembrane helices M4, M5, M6 and M8 of the SR Ca^{2+}-ATPase, corresponding to Glu-309 and Asp-800 in M4 and M6 respectively [52]. The fact that these two residues correspond to site II also suggests that site II may be more fundamental to the operation of the SR Ca^{2+}-ATPase than site I, and that occupancy of site II is required to generate the active conformation of the Ca^{2+}-ATPase.

That Glu-309 at site II is particularly important is suggested by experiments in which this residue was replaced by Asp [53]. The affinity for Ca^{2+} in Ca^{2+}-dependent phosphorylation by ATP was little altered by the mutation, but CrATP was unable to occlude significant levels of Ca^{2+} [53]. This suggests that Glu-309 plays a role in trapping Ca^{2+} in the ATPase as well as in simply binding Ca^{2+}, with the smaller Asp residue being less good at trapping. The rate of phosphorylation by ATP was also much reduced by the Glu-309 to Asp mutation, again suggesting that site II is important in generating the active conformation of the ATPase required for phosphorylation.

Mutation of residues close to the Ca^{2+} binding residues also blocks Ca^{2+} binding [54], presumably through secondary effects of packing. The effects of mutating the large hydrophobic residues Phe-760, Tyr-763 and Leu-764 are of interest, since these lie immediately above site I, on the cytoplasmic side of the membrane. Whereas mutation of Phe-760 and Leu-764 led to a reduction in Ca^{2+} affinity, mutation of Tyr-763 to Gly gave an uncoupled mutant in which Ca^{2+} transport was uncoupled from hydrolysis of ATP [54,55]. Mutation of Lys-758 also gives an uncoupled mutant [45]. It could be that mutation of Tyr-763 or Lys-758 opens a pathway for the passive leak of Ca^{2+} through the ATPase, from the lumenal to the cytoplasmic side. It is more likely, however, that mutation of these residues allows Ca^{2+} to be released from the phosphorylated ATPase to the cytoplasmic side of the membrane, an example of 'true' uncoupling.

The pathway for Ca^{2+} binding

The locations of all the acidic residues in the transmembrane region of the Ca^{2+}-ATPase are shown in Figure 5(A), together with those in the cytoplasmic and lumenal regions close to the membrane surface. The surface of the membrane can be defined in a number of ways. The transmembrane region of a membrane protein is usually taken to correspond to the region spanning the hydrocarbon core of the lipid bilayer between the lipid backbone regions on the two sides of the membrane (see [15]). Thus the surface of the membrane will be taken as the plane through the lipid backbone region. Trp residues are frequently found close to the membrane–water interfaces of membrane proteins, either in the lipid headgroup region or penetrating into the hydrocarbon core [15].

The membrane–water interface on the cytoplasmic side of the Ca^{2+}-ATPase can be identified with some certainty, since a clear ring of Trp residues can be seen on the cytoplasmic side (Figure 5C). Furthermore, seven acidic residues (Glu-51, Glu-55, Glu-

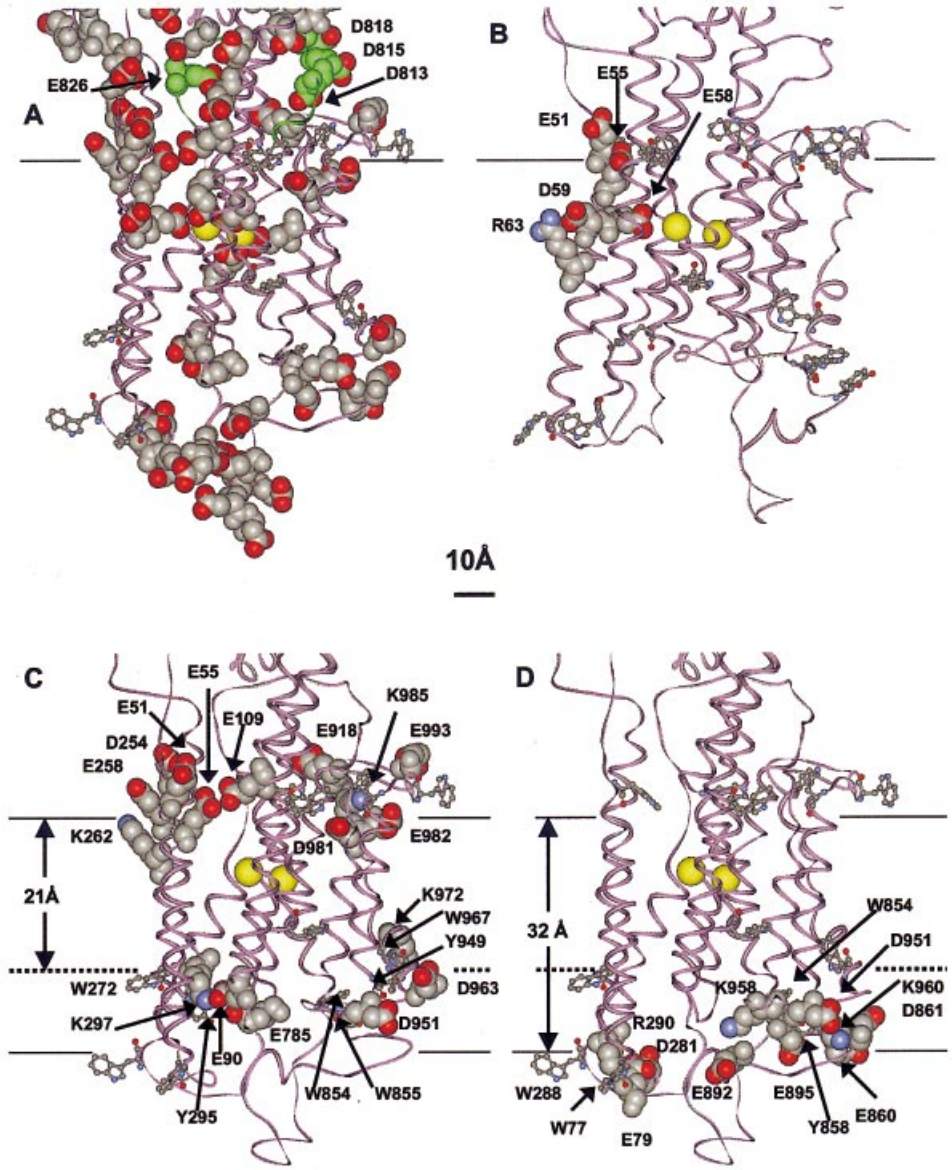

Figure 5 Acidic residues in the transmembrane region of the Ca^{2+}-ATPase and close to the cytoplasmic and lumenal surfaces

Trp residues are shown in ball-and-stick representation, and acidic residues are shown in space-fill representation. The two Ca^{2+} ions are shown in yellow. (**A**) Positions of the acidic residues. Acidic residues in the M7–M8 loop are shown in green. The horizontal line shows the likely position of the cytoplasmic surface. (**B**) A different orientation of the Ca^{2+}-ATPase, making clear the locations of Asp-59 and Arg-63 in transmembrane α-helix M1 pointing out into the lipid bilayer. Also shown are the other acidic residues in M1, i.e. Glu-51, Glu-55 and Glu-58. (**C**, **D**) Ca^{2+}-ATPase in the same orientation as in (**A**), showing charged residues that define the likely position of the cytoplasmic surface (**C**), and two possible locations for the lumenal surface, 21 Å (**C**, broken line) or 32 Å (**D**, solid line) from the cytoplasmic surface.

109, Asp-254, Glu-258, Glu-918 and Glu-993) are located with their carboxy groups close to the surface defined by the ring of Trp residues. Since there are no basic residues located in the structure close to these acidic residues, it is unlikely that these residues reside within the hydrophobic core of the membrane. A basic residue (Lys-262) also points up to this surface from M3, helping to define the surface (Figure 5C).

Figure 5(A) shows that the ATPase contains no immediately obvious channels leading from the cytoplasmic surface to the pair of high-affinity binding sites. In this respect the Ca^{2+}-ATPase is very unlike the porins [56] and ion channels such as the potassium channel KcsA [57], where the pathway across the membrane is obvious in the structure. Identification of the entry and exit pathways for Ca^{2+} in the Ca^{2+}-ATPase is made more difficult by the likelihood that the structure of the Ca^{2+} binding sites differs in the absence and presence of Ca^{2+} because of charge repulsion between the four carboxy groups in the absence of Ca^{2+}.

Running along the bottom of the P domain, close to the cytoplasmic surface, is the M7–M8 loop, which contains four acidic residues (Figure 5A). Mutation of these acidic residues has been shown to result in reduced affinity for Ca^{2+}, leading to the suggestion that the loop could be a direct part of the Ca^{2+} binding site [58]. However, the location of these residues makes

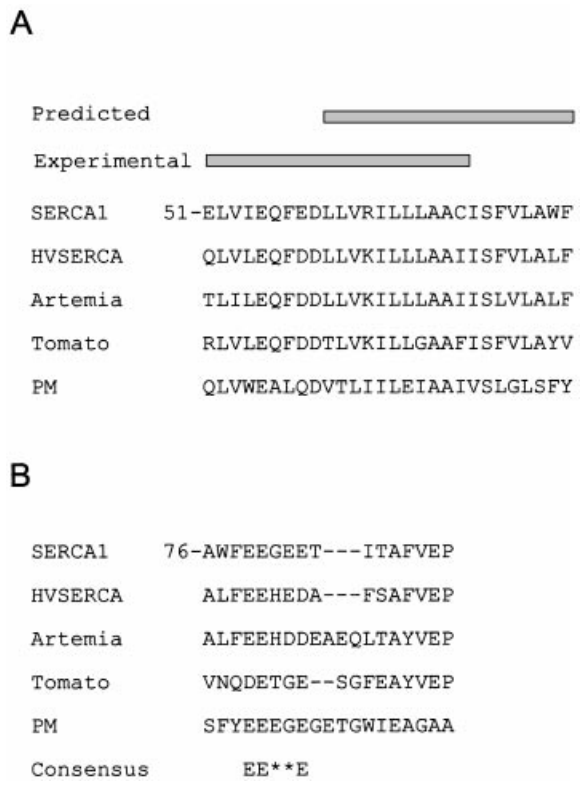

Figure 6 Sequence comparisons for Ca^{2+}-ATPases

(**A**) Comparison of the sequences of the first transmembrane α-helices. The bars represent the predicted and experimental locations of the helix. (**B**) Comparison of the sequences of the M1–M2 loop. Sequences are shown for the following Ca^{2+}-ATPases: SERCA1, fast-twitch rabbit skeletal muscle [121]; HVSERCA, *Heliothis virescens* [122]; *Artemia* [123]; tomato [124]; PM, human plasma membrane [125].

their direct involvement in Ca^{2+} binding very unlikely; the effects of mutation presumably follow indirectly from changes in the conformation of the M7–M8 loop. Toyoshima et al. [3] suggested a pathway for Ca^{2+} entry leading from the cytoplasmic surface along a path almost perpendicular to the membrane surface to site II, between transmembrane α-helices M4 and M6, involving backbone oxygens of the unwound M4 between Glu-309 and Pro-312. However, an alternative pathway is suggested by the unexpected nature of the first transmembrane α-helix of the Ca^{2+}-ATPase, M1.

Transmembrane α-helix M1 starts at about Glu-51 rather than at Leu-60, as assumed previously (Figure 6). M1 therefore contains four acidic residues and one basic residue at its N-terminal end, which explains its misdiagnosis in hydropathy plots. Of these charged residues, Glu-58, Asp-59 and Arg-63 are located within the hydrophobic core of the bilayer, and Glu-51 and Glu-55 are located at the surface (Figure 5B). Glu-58 is oriented towards the Ca^{2+} ion bound to site II. Asp-59 is oriented pointing out into the surrounding lipid bilayer. Location of charged groups in lipid bilayers is highly unfavourable energetically, but Asp-59 is stacked against Arg-63 so that they presumably form an ion pair (Figure 5B).

Of the four acidic residues in M1, all but Glu-51 are conserved in the family of ER/SR Ca^{2+}-ATPases (Figure 6), suggesting that this cluster of charged residues is functionally important. The importance of these residues is also suggested by the fact that two of the negatively charged residues (equivalent to Glu-55 and Asp-59) are conserved in the plasma membrane Ca^{2+}-ATPase, paralleling the observed conservation of two of the four acidic residues at the pair of high-affinity sites in the SR Ca^{2+}-ATPase [52]. The location of Glu-58 close to the Ca^{2+} ion bound to site II (Figure 3) means that this residue is likely to be able to 'sense' whether or not site II is occupied by Ca^{2+}, with the conformation of this region of M1 possibly changing on Ca^{2+} binding. This could be important, since the ATPase has not only to provide a pathway for entry of Ca^{2+} to the high-affinity pair of sites, but it must also be possible to close off this pathway following phosphorylation, so that Ca^{2+} is not lost from the phosphorylated ATPase to the cytoplasm.

M1 could possibly provide the entry pathway leading to the Ca^{2+} binding sites. As shown in Figure 7, a short channel, lined by Glu-58, leads between Glu-109 and Glu-55 on the membrane surface to site II buried within the lipid bilayer. This channel is largely blocked by Glu-309 in the E1′Ca_2 form, but it is possible that, in the Ca^{2+}-free form, Glu-309 is located to leave free access to site II. This pathway is on the opposite side of residues 309–312 in M4 suggested by Toyoshima et al. [3] to line the access pathway (see Figure 7).

Binding of Ca^{2+} to the cytoplasmic sites is ordered; binding of the second Ca^{2+} ion prevents dissociation of the first Ca^{2+} ion [59–62]. This is what would be expected if the Ca^{2+} ions were to bind within a channel-like structure, where binding of the second Ca^{2+} ion to the 'outer' of the two sites would trap the first Ca^{2+} ion bound in the 'inner' site. In such a structure, a Ca^{2+} ion would have to pass through site II in order to reach site I. This would be possible if site II were not properly formed in the absence of Ca^{2+} at site I, explaining the co-operativity of Ca^{2+} binding to the ATPase.

Another feature of the Ca^{2+} binding sites that has to be explained is that dissociation of Ca^{2+} is slow; it has been suggested that the binding and dissociation of Ca^{2+} are controlled by a conformational change in a 'gating' site [25,62–64]. The rate of binding of Ca^{2+} is dependent on pH, and is also affected by Mg^{2+} and K^+, suggesting that H^+, K^+ and Mg^{2+} can all bind to the gating site [62–64]. In the structure of E1′Ca_2, the gate is probably closed. Opening of the gate could correspond to a twisting of the N-terminal end of M1 (which is somewhat unwound) to relocate the acidic residues in M1, providing a pathway for Ca^{2+} to reach the cytoplasmic pair of sites, together with a relocation of Glu-309. A conformation for helix M1 in E2 similar to that in E1′Ca_2 could explain why Ca^{2+} was unable to bind to the cytoplasmic sites in the E2 conformation; it is possible that interaction of the Ca^{2+} ion bound at site II with Glu-58 enables the gate to open in the E1′Ca_2 conformation, but that, in the absence of this Ca^{2+} ion (in the E2 state), the gate is locked shut.

Arguing against an important role for the acidic residues in M1 are the results of mutagenesis experiments. Mutation of Glu-55, Glu-58 and Asp-59 alone has been shown to have no effect on the rate of accumulation of Ca^{2+}, measured in the presence of oxalate to precipitate Ca^{2+} within the lumen of the microsomes; simultaneous mutation of all three residues led to a 30% decrease in the rate of accumulation of Ca^{2+} [65]. However, as long as the mutations did not block the entry pathway, it is not clear that a large effect would be expected from mutations under conditions of high external Ca^{2+} concentrations. There seem to be no reported studies of mutagenesis of Glu-51.

Phosphorylation of the ATPase

It has been shown using chemical labelling that the adenine and γ-phosphate moieties of ATP bind to separate domains on the

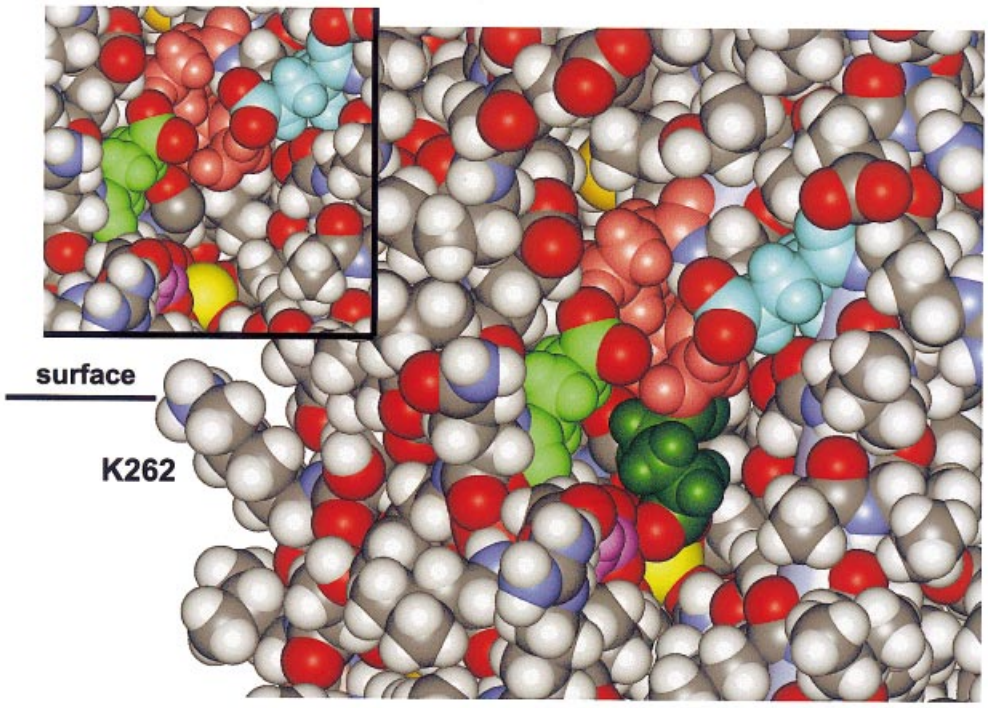

Figure 7 Possible pathway for Ca^{2+} binding

The view is from the side, in an orientation similar to that in Figure 5(A). The membrane surface is indicated by the horizontal line. Important acidic residues are coloured as follows: Glu-55, light green; Glu-58, lilac; Glu-109, light blue; Glu-309, dark green. The Ca^{2+} ion bound at site II is shown in yellow. Residues 310–312 are shown in brown. The bound Ca^{2+} ion at site II is clearly visible at the bottom of a short channel lined by Glu-58. The inset shows the same view, but with Glu-309 removed, showing how Glu-309 sits above the Ca^{2+} ion at site II.

ATPase, the N and P domains respectively. Analogues of ATP with reactive groups on the rings invariably label residues in the N domain; these analogues block phosphorylation by ATP, but not by acetyl phosphate or P_i [6]. However, if the reactive group is close to the γ-phosphate, then the residues labelled are in the P domain and the modified ATPase cannot be phosphorylated by either ATP or P_i [6].

The catalytically active E1″Ca_2·ATP conformation can be produced by pathways in which either Ca^{2+} or ATP binds first to the ATPase (Scheme 1) [23,27,28]. In the pathway in which Ca^{2+} binds first to give E1′Ca_2 followed by binding of ATP, a slow ($k_3 = 220\ s^{-1}$) conformation change leads to the active state. In the other pathway, ATP binds first, followed by Ca^{2+} and a slow ($k_6 = 70\ s^{-1}$) conformational change to give the active state [23]. By either pathway, the active state can only be reached following the binding of both ATP and Ca^{2+}. Binding of MgATP is relatively slow in either pathway, with on and off rates respectively of $10^7\ M^{-1}\cdot s^{-1}$ and $120\ s^{-1}$ for the Ca^{2+}-bound form, and $5.3 \times 10^6\ M^{-1}\cdot s^{-1}$ and $24\ s^{-1}$ for the Ca^{2+}-free form [23]. The relatively low rates of MgATP binding shows that binding is not simply an encounter process but, rather, must involve a conformational change on the ATPase.

The structure of the Ca^{2+}-ATPase crystallized in the presence of Ca^{2+} and the nucleotide 2′,3′-*O*-(2,4,6-trinitrophenyl)-AMP (TNP-AMP) shows TNP-AMP binding to the surface of the N domain, more than 25 Å away from Asp-351 (Figure 8) [3]. TNP-AMP is presumed to bind to the nucleotide binding site, since binding of analogues of TNP-AMP is competitive with binding of ATP [66]; in addition, Lys-515 and Lys-492 are close to the bound TNP-AMP, and labelling studies have shown that these two residues are at the active site. Surprisingly, the TNP-AMP binding site is distinct from that assigned previously to the non-phosphorylating ATP analogue CrATP on the basis of electron microscopy studies [67]; this is particularly clear in the figures presented in [68].

Binding of ATP to the Ca^{2+}-ATPase in the presence of Ca^{2+} results in a large conformational change to bring the terminal phosphate of the bound ATP close to Asp-351. However, the structure of the ATPase with bound Ca^{2+} and TNP-AMP is not significantly different from that in the absence of TNP-AMP [3]. Presumably the γ-phosphate of ATP is required to bring about the conformational change, and its absence from TNP-AMP explains the lack of any significant conformational change on binding of this analogue. The nature of the conformational change on the Ca^{2+}-ATPase following the binding of Ca^{2+} and ATP has been deduced by comparing the crystal structure of E1′Ca_2 with low-resolution electron microscopy structures of the Ca^{2+}-ATPase [3]. The E1′Ca_2 conformation corresponds to the form identified as the open form in electron microscopic studies, because of the presence of clear, separate domains on the cytoplasmic side [39]. In contrast, crystallization in the absence of calcium, but in the presence of vanadate, gives a closed form of the ATPase in which packing of the cytoplasmic domains is more compact, which is believed to be similar to the E2 or E2P forms of the ATPase [39]. Toyoshima et al. [3] showed that the closed form could be fitted reasonably well to the X-ray structure by whole domain movements of the cytoplasmic domains. A 90° rotation of the A domain brings the highly conserved T^{181}GES loop into the phosphorylation site. A 20° rotation of the N domain partially closes the gap between the N and P domains,

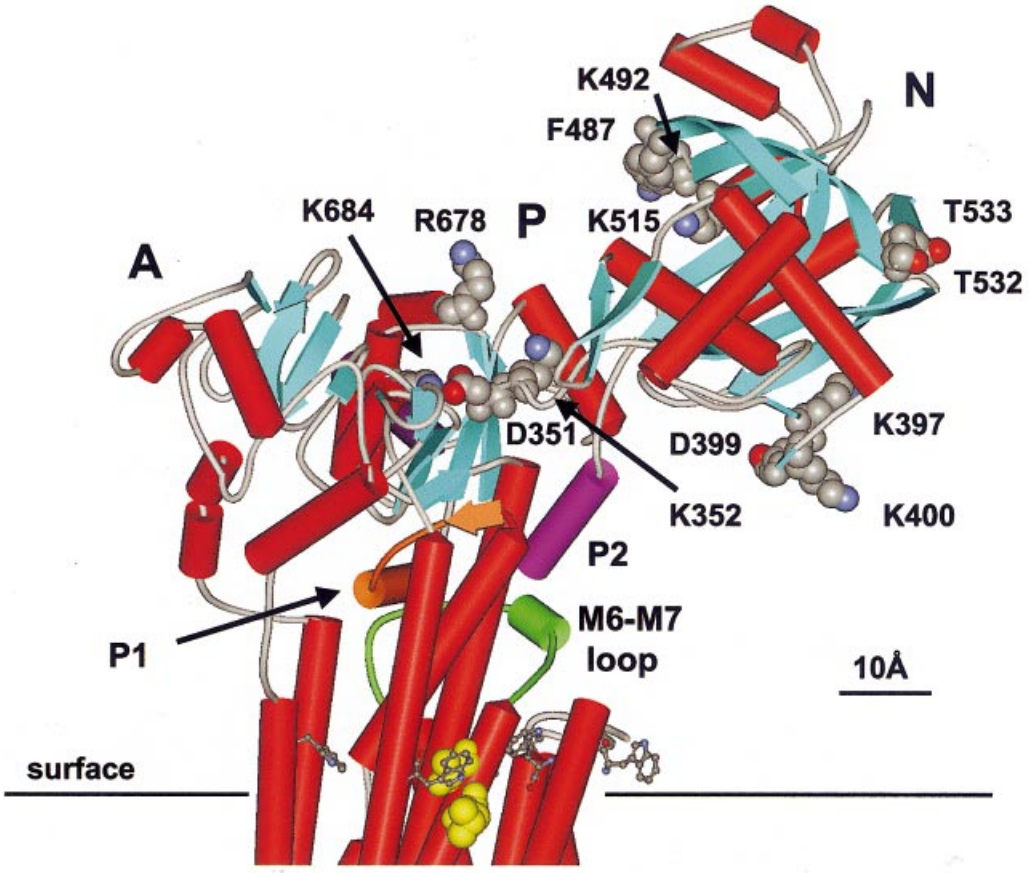

Figure 8 Cytoplasmic domains of the Ca^{2+}-ATPase in a view from the side

Residues shown to be important in binding MgATP are indicated. The two helices P1 and P2 in the P domain are marked, together with the M6–M7 loop believed to be important in coupling hydrolysis of ATP to transport of Ca^{2+}. Also indicated are the residues in the N domain ($K^{397}NDKPV^{402}$) believed to be important in interaction with the cytoplasmic domain of phospholamban, and residues Leu-802 and Thr-805 (shown in yellow) in the transmembrane region of the ATPase which are believed to be important in interaction with the transmembrane domain of phospholamban.

although a distance of 15–20 Å still remains between the nucleotide binding site and Asp-351. Complete closure of the two domains is prevented by a density ascribed to decavanadate ($V_{10}O_{28}^{6-}$), bound to a highly positively charged groove containing Arg-489, Lys-492 and Arg-678; binding to such a site could explain inhibition of ATPase activity by decavanadate. A smaller vanadate oligomer also appears to be bound close to Asp-351. The relationship between the P domain and the transmembrane α-helices M4 and M5 also changes, and the large movement of the A domain requires changes in the orientations of helices M1–M3 [3]. The loop connecting helices M6 and M7 moves with the P domain to a position higher above the membrane surface than in E1′Ca_2 [3]. These conformational changes are possible because of the flexible connection between the P and N domains, and between the A domain and the rest of the protein.

Any conformational alterations in the P domain during these changes must be relatively small. Fluorescence energy transfer measurements between labelled residues on the Ca^{2+}-ATPase and fluorescently labelled phospholipids show that the heights of Cys-344, Cys-670 and Cys-674 hardly change between the Ca^{2+}-bound E1 state and the vanadate-bound E2 state [69]. These measurements also show that Glu-439, located at the end of the N domain closest to the P domain, and Lys-515 do not move significantly with respect to the membrane surface between E1 and E2 [69]. The relative heights of these residues above the membrane surface agree well with the crystal structure, although the absolute values are overestimated by approx. 20 Å [69]. This overestimate of absolute heights can be attributed to the method of analysis that treats the fluorescently labelled lipid as being distributed randomly on a plane. However, the membrane protein will exclude lipids from a volume of the bilayer corresponding to the volume occupied by the protein itself, and so will effectively 'cast a shadow' on to the plane of the membrane, in which there will be no labelled lipid to take part in fluorescence energy transfer. The effect will be to reduce the observed level of energy transfer, so that the usual methods of analysis will give a maximum value for the height above the bilayer surface. The method of Gutierrez-Merino et al. [70] accounts for the effect of the protein and, with a diameter of the transmembrane region of the ATPase plus the first shell of lipid of approx. 60 Å, gives heights of residues above the surface that are in close agreement with the crystal structure (A. G. Lee and J. M. East, unpublished work).

The P domain of the Ca^{2+}-ATPase consists of residues from about Asn-330 to Asn-359 connected to S4, and a larger region from Lys-605 to Asp-737 connected to S5 [3]. These residues

form a seven-stranded parallel β-sheet surrounded by eight short α-helices in a typical Rossmann fold. Between the end of the first β-strand (Asp-351) and the start of the first α-helix of the Rossmann fold (Glu-606) is the inserted N domain. Identification of residues important in phosphorylation has been helped enormously by the realization that the P-type ATPases are members of the HAD superfamily of hydrolases [5]. Particularly useful comparisons have been made with the structure of the protein FixJ, a member of the HAD family. The structure of FixJ has been determined in both the unphosphorylated and phosphorylated states. On phosphorylation of the Asp residue equivalent to Asp-351 in the Ca^{2+}-ATPase, a conserved Lys residue, equivalent to Lys-684 in the Ca^{2+}-ATPase, moves to form a salt bridge with the phosphate group [71]. Whereas in most members of the HAD family the conserved Lys residue is located in a turn preceding an α-helix, in the Ca^{2+}-ATPase, Lys-684 is part of an α-helix which, in the unphosphorylated ATPase, is co-ordinated to Asp-351 (Figure 8). Thus, although Lys-684 might re-orient on phosphorylation to form a salt bridge to the phosphate group, this is unlikely to result in a change in the backbone conformation around Lys-684 of the type seen in FixJ, because of the stability of α-helices. More likely is a shift in the relative positions of the loop containing Asp-351 and the helix containing Lys-684. This movement could, in turn, lead to changes in the packing of the transmembrane α-helices, as described below.

The segment to the C-terminal side of Asp-351 (D^{351}KTGTLT^{357}) is highly conserved in the P-type ATPases. Lys-352, Thr-355, Leu-356 and Thr-357 have been shown to be critical for Ca^{2+} transport and for phosphorylation [72]. Mutation of Lys-352 decreased the affinity for MgATP, suggesting a favourable electrostatic interaction between the lysine and the phosphate [73]. Of course, mutation of Asp-351 itself leads to loss of activity. However, removal of the negative charge on Asp-351 led to an increased affinity for MgATP, particularly in the presence of Ca^{2+} [73]. This is in contrast with the wild-type protein, for which it has been estimated from rates of binding and dissociation of MgATP that binding of Ca^{2+} has little effect on the affinity for MgATP [74]. The effects of mutation of Asp-351 suggest strong electrostatic repulsion between the γ-phosphate of ATP and Asp-351 in the wild-type protein. This may serve to prevent the formation of a large energy well within the reaction cycle (i.e. Asp-351 could destabilize $E1''Ca_2 \cdot ATP$ relative to $E2PCa_2$).

Residues around the nucleotide binding site on the Ca^{2+}-ATPase have been identified from chemical labelling experiments. The crystal structure in the presence of TNP-AMP shows nucleotide binding near to Phe-487, Lys-515 and Lys-492 (Figure 8); the binding pocket for TNP-AMP is positively charged due to residues Arg-489, Lys-492, Lys-515 and Arg-560 [3]. Labelling of Lys-515 with FITC blocks ATP binding without affecting phosphorylation by P_i, and Lys-515 has long been considered a marker for the ATP binding site [75]. The crystal structure of the Ca^{2+}-ATPase shows Lys-515 deep in the pocket around the adenine moiety of bound TNP-AMP [3]. Rather surprisingly, mutation of Lys-515 to Ala inhibits both ATP- and acetylphosphate-supported transport of Ca^{2+} [72].

Adenosine triphosphopyridoxal labels Lys-684 in the P domain in the presence of Ca^{2+}, and both Lys-684 and Lys-492 in the absence of Ca^{2+}, consistent with a change in the relative positions of these two residues on binding of Ca^{2+} [76,77]. Lys-492 and Arg-678 in the P domain are cross-linked by glutaraldehyde [78] in an ATP-protectable manner, again consistent with a conformational change bringing the N and P domains close together. Cross-linking of Lys-492 to Arg-678 with glutaraldehyde allowed ATP-dependent occlusion of Ca^{2+}, but completely blocked release of Ca^{2+} to the lumen [78,79]. As can be seen in Figure 8, Arg-678 is located on the top surface of the P domain, pointing towards the N domain.

McIntosh and Woolley [80] have shown that the γ-phosphate of an ATP analogue [2′,3′-*O*-(2,4,6-trinitrophenyl)-8-azido-ATP] covalently linked to Lys-492 is able to phosphorylate Asp-351, albeit at a low rate. This implies that Lys-492 and Asp-351 must be separated by approx. 14 Å in the Ca^{2+}-bound complex. Further, it implies that Lys-492 must be close to the adenyl moiety of the nucleotide in the complex.

Ca^{2+} transport

In the four-site model for transport, transport corresponds to the transfer of the two bound Ca^{2+} ions from the pair of cytoplasmic sites to the pair of lumenal sites. In the alternating four-site model, Ca^{2+} ions are released from the pair of transport sites following phosphorylation of the ATPase, linked to closure of the pair of lumenal sites (Figure 4). Unfortunately, the crystal structure of $E1'Ca_2$ provides only limited information about the identity of the lumenal pair of sites for Ca^{2+}. The lumenal pair of sites are not occupied in the crystal, and the low affinity (millimolar) of the sites for Ca^{2+} means that they are likely to be less easy to identify than the high-affinity sites. It is also difficult to decide where the lumenal face of the membrane should be drawn; there is no clear ring of Trp residues on the lumenal side of the membrane, of the type found on the cytoplasmic side (Figure 5). Further, it has been suggested that the hydrophobic thicknesses of the E1 and E2 conformations of the Ca^{2+}-ATPase are different [81,82]. The thickness of the surrounding lipid bilayer affects the E1/E2 equilibrium, with dimyristoleoyl phosphatidylcholine (dimyristoleoyl-PC) favouring the E1 conformation and dioleoyl-PC favouring the E2 conformation; increasing the chain length of the lipid beyond dioleoyl-PC had no additional effect on the E1/E2 equilibrium [81,82].

The locations of Asp-963 and Lys-972 without oppositely charged partners on the lumenal side of the membrane and the salt bridge between Glu-90 and Lys-297 define a plane close to that defined by Trp-272, Trp-854, Trp-967, Tyr-295 and Tyr-949, which could represent the lumenal surface (Figure 5C). This would define a hydrophobic thickness for the bilayer of approx. 21 Å, much lower than the values that have been estimated for other membrane proteins whose high-resolution structures have been determined [57,83–88], which lie in the range 25–33 Å. However, a hydrophobic thickness for the E1 conformation of the ATPase of 21 Å would match the thickness of a bilayer of dimyristoleoyl-PC, which is approx. 23 Å [89,90]. For the E2 conformation to match the thickness of a bilayer of dioleoyl-PC, the lumenal surface in the E2 conformation would have to be approx. 30 Å from the cytoplasmic surface. A plane 32 Å from the cytoplasmic surface can be defined, as shown in Figure 5(D), containing Trp-77, Trp-288, Tyr-858, the acidic residues Glu-79, Asp-281, Asp-861, Glu-892, Glu-895 and Asp-951, and the basic residues Arg-290 and Lys-960.

The defining features of the hydrophobic thickness in the $E1'Ca_2$ conformation are the M5–M6 and M9–M10 loops, which are much closer to the cytoplasmic surface than are the other lumenal loops. A relocation of these two loops or a movement of the transmembrane α-helices could result in an increase in the effective transmembrane length for helices M5, M6, M9 and M10. Large changes in the transmembrane region of the Ca^{2+}-ATPase on phosphorylation are suggested by a comparison of electron micrographs of the open and closed forms of the Ca^{2+}-ATPase [39].

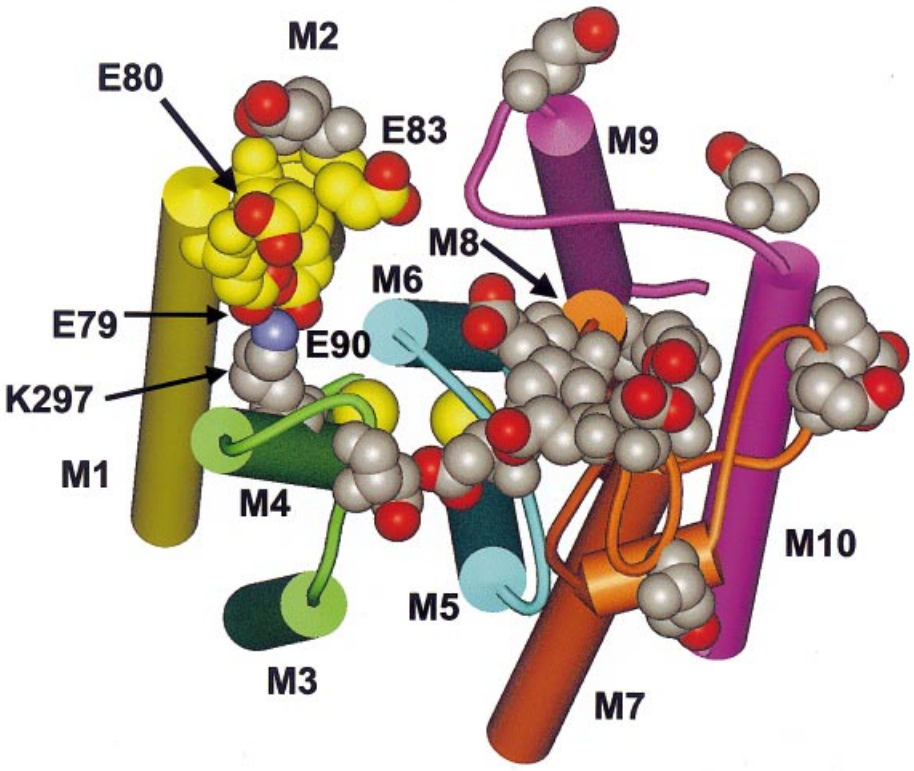

Figure 9 Acidic residues in loops on the lumenal side of the membrane

Shown is an end-on view from the lumenal surface. The two bound Ca^{2+} ions are shown in yellow. Colours are as follows: M1–M2, yellow; M3–M4, green; M5–M6, blue; M7–M8, brown; M9–M10, purple. The acidic residues are shown in space-fill format; the conserved residues Glu-79, Glu-80 and Glu-83 are shown in yellow. Lys-297, which forms an ion pair with Glu-90, is also shown.

The only acidic residues on the lumenal side of the membrane are located in the loops connecting the transmembrane α-helices; chemical labelling experiments have shown that acidic residues on the lumenal side of the membrane are important for function [91]. The most highly conserved of the loops on the lumenal side of the membrane is the M1–M2 loop (Figure 6). The sequence (D/E)EXX(D/E) is conserved in all the Ca^{2+}-ATPases, including the plasma membrane Ca^{2+}-ATPase. In addition, the sequence (F/Y)VEP is found at the lumenal end of helix M2 in all except the plasma membrane Ca^{2+}-ATPase. These residues form a cluster around the N-terminal end of M2 (Figure 9). The conservation of these acidic residues makes them a possible candidate for the lumenal binding sites for Ca^{2+}. Other acidic residues are located in loop M7–M8, the largest of the lumenal loops in the SR Ca^{2+}-ATPase, but the loop is poorly conserved and is much shorter in the plasma membrane Ca^{2+}-ATPase [2]. An acidic residue (Glu-785) is also found in loop M5–M6, but again this loop shows no obvious conservation in the family of Ca^{2+}-ATPases [2].

Since there is no obvious channel leading from the cytoplasmic pair of sites to the lumenal surface, release of Ca^{2+} must occur as a result of a major conformational change, perhaps involving an opening up of the interface between helical bundles M1–M4 and M5–M10, allowing access to the lumen. During the transport process, the order of binding of the two Ca^{2+} ions to the cytoplasmic pair of sites is lost, so that it is no longer possible to distinguish between the first and second Ca^{2+} ion to bind [92,93]. It has also been shown that, at least under some conditions, release of Ca^{2+} from the lumenal sites is sequential [94,95].

In terms of the four-site model for transport, the two Ca^{2+} ions could become randomized during the transfer between the cytoplasmic and lumenal sites. The four-site model would also require that the rate of transfer of the two Ca^{2+} ions to the pair of lumenal sites be relatively high, since it is simultaneous with phosphoryl transfer ($E1''Ca_2 \cdot ATP \rightarrow E2PCa_2$), and phosphoryl transfer is known to be fast ($\geqslant 1000\ s^{-1}$ [28]). The rate of dissociation of Ca^{2+} from the lumenal sites on E2P is known to be relatively low, with a rate constant of approx. $20\ s^{-1}$, suggesting that a significant conformational change is involved in release [94]. In contrast, dissociation of Ca^{2+} from the lumenal sites on the unphosphorylated ATPase must be faster than a rate of $220\ s^{-1}$ [96]. This is because the presence of lumenal Ca^{2+} has no effect on the rate of phosphorylation of the ATPase by ATP, meaning that the rate of dissociation of Ca^{2+} from the lumenal sites on the unphosphorylated protein must be higher than the rate of the conformational change that limits the rate of the phosphorylation reaction, which is $220\ s^{-1}$ [96].

The kinetics of transport can be explained in a rather more convincing way in terms of the alternating four-site model. In the alternating four-site model, if either of the two bound Ca^{2+} ions can enter the release channel first, the order of the two Ca^{2+} ions would be lost. The location of the release channel is rather uncertain, but Toyoshima et al. [3] identified a ring of oxygen atoms between M3, M4 and M5 with bound water molecules that they suggested could make up the exit pathway. In the alternating four-site model, phosphorylation of the ATPase would lead to a conformational change at the pair of transport sites and a closing of the lumenal pair of sites, which could be fast

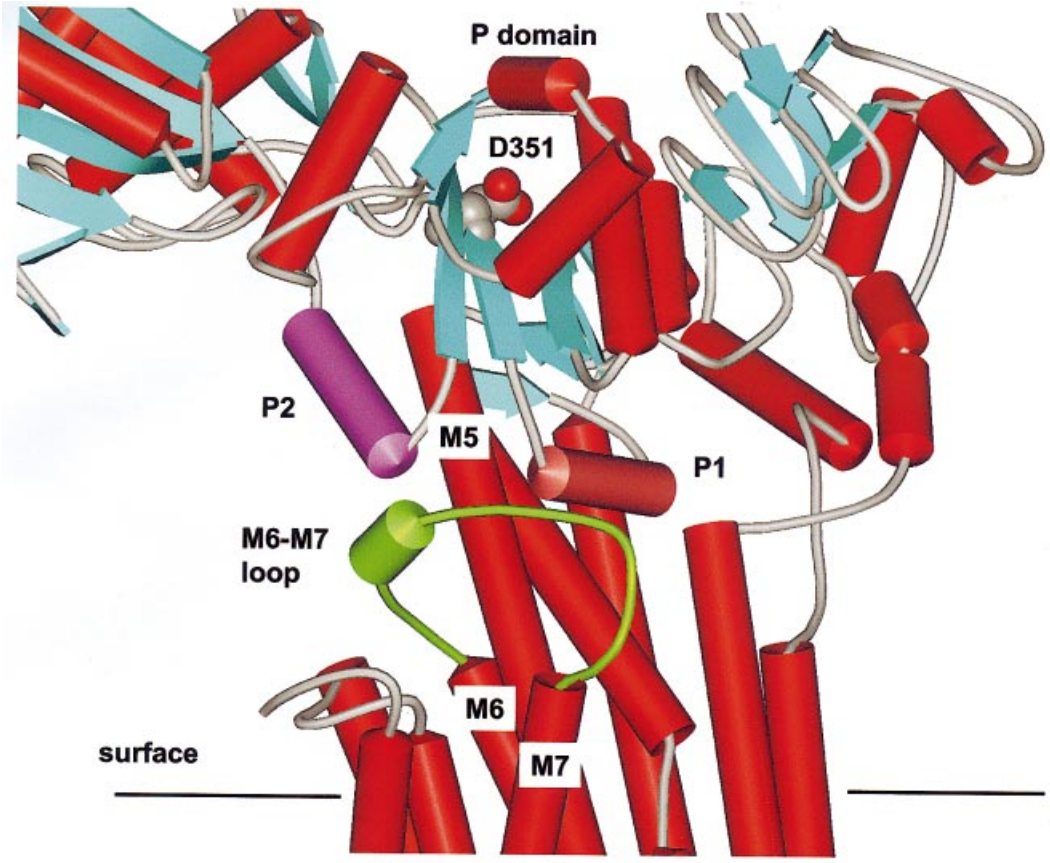

Figure 10 Link between the P domain and the transmembrane α-helices

Helices P1 (browny red) and P2 (purple) in the P domain contact the M6–M7 loop (green).

($\geqslant 1000\ s^{-1}$). The slow step required for release of Ca^{2+} would correspond to the major conformational change in the ATPase required to open up the release pathway from the pair of transport sites to the lumenal surface of the ATPase; since this represents a major change in structure, it is likely to be slow. The required high rate of dissociation of Ca^{2+} from the lumenal pair of sites on the unphosphorylated ATPase ($> 220\ s^{-1}$) would not be unexpected, given the low affinity of these sites. It might be noted that the affinities of the lumenal pair of sites and of the pair of transport sites on the phosphorylated ATPase are known to be slightly different; the pair of transport sites on E2P have a slightly higher affinity for Ca^{2+} than the lumenal pair of sites on E2 [21]. In contrast, the affinities of the lumenal pair of sites for Ca^{2+} must be very similar in the E1 and E2 conformations, since, as described above, the presence of lumenal Ca^{2+} does not affect the E1/E2 equilibrium.

Experiments in which acidic residues on the lumenal side of the membrane were mutated are in somewhat better agreement with the alternating four-site model for transport than with the four-site model. Mutation of the acidic residues in the M1–M2 loop had no effect on the rate of accumulation of Ca^{2+} measured in the presence of oxalate as a precipitating agent for Ca^{2+} [65]. In the four-site model, if these residues make up the lumenal pair of sites from which the transported Ca^{2+} is released, then their mutation might have been expected to lead to a decrease in the rate of transport. Although various explanations for the lack of any observed effect could be put forward, these experiments do tend to favour the alternating four-site model, since, in this model, mutation of residues at the lumenal pair of sites would not be expected to affect the rate of transport.

Linking phosphorylation to transport

The region of the Ca^{2+}-ATPase responsible for linking changes at the phosphorylation site with changes in the Ca^{2+} binding sites is the stalk region. As shown in Figure 10, the loop between transmembrane helices M6 and M7 (Gly-808 to Gly-831) is located in the stalk region, running along the bottom of the P domain. As described above, comparison of the crystal structure of E1′Ca_2 with the low-resolution structure of the vanadate-bound ATPase suggests that the M6–M7 loop moves to a position higher above the surface in the vanadate-bound state, believed to be similar to the phosphorylated state [3]. The M6–M7 loop has conserved features [97]. It contains six Pro residues, four of which are present as pairs. Contacting the loop are two helices of the P domain, P1 (Leu-336 to Cys-344) and P2 (Glu-606 to Ala-617), as shown in Figure 10. The P1 helix (V^{339}ETLG) is conserved in cation P-type ATPases [1]. Cys-344 at one end of helix P1 abuts directly against Pro-821 and Pro-824 (Figure 11). Helix P1 has the appearance of a piston that can press against the stirrup-like M6–M7 loop, linking the P domain and the transmembrane α-helices. Since P1 is part of the N-terminal region of the P domain that contains Asp-351, movement of P1 on phosphorylation could move the M6–M7 loop,

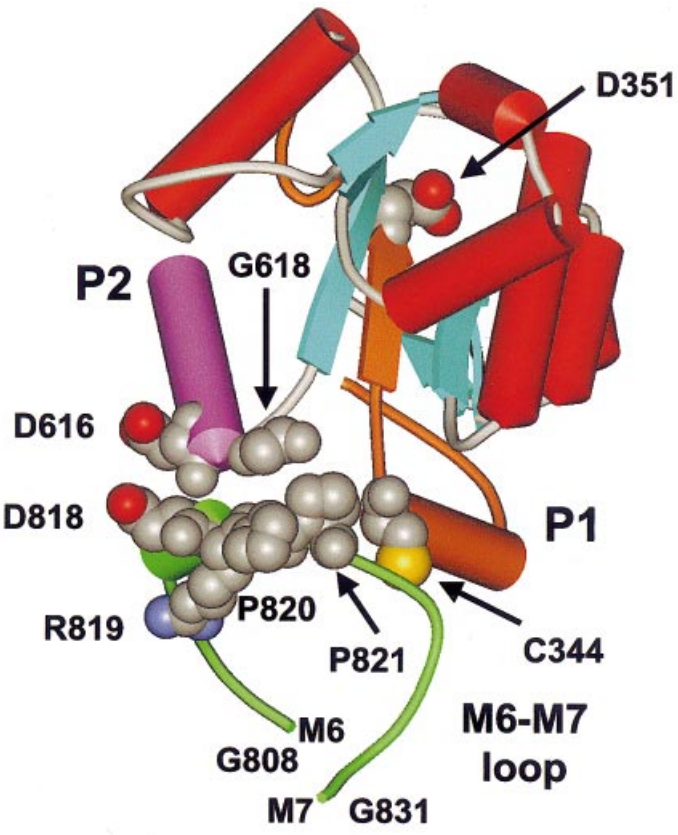

Figure 11 Contact between helices P1 and P2 and the M6–M7 loop

The Figure shows the residues at the tips of helices P1 and P2 and in the M6–M7 loop that are in contact.

and thus move helices M6 and M7. Movement of helices M6 and M7 could, in turn, lead to movement of other transmembrane α-helices. Since the ligands for Ca^{2+} at the high-affinity binding sites are located on separate helices, any changes in the packing of the helices would result in large changes in the affinity for Ca^{2+}. In a similar way, binding of Ca^{2+} to the cytoplasmic pair of sites could lead to changes in the packing of the transmembrane α-helices, and through the M6–M7 loop and helix P1, signal to the P domain that Ca^{2+} had bound to the ATPase. Although, at present, the details of the proposal are largely speculative, it does at least seem highly likely that the link between changes in the phosphorylation and transmembrane domains is purely mechanical.

Mutation of acidic residues in the M6–M7 loop resulted in reduced affinity for Ca^{2+} and led to the suggestion that the loop could be a direct part of the Ca^{2+} binding site [58]. The crystal structure shows that this is unlikely to be the case. It is more likely that the mutations have an indirect effect through conformational changes in the loop and neighbouring parts of the structure. Mutation of Pro-811 and Pro-812 had no effect on the function of the ATPase, but mutation of Pro-820 and Pro-821 reduced Ca^{2+} affinity, with mutation of Pro-821 having the largest effect [58]. As shown in Figure 11, Pro-821 contacts Cys-344 at the tip of helix P1.

Helix P2 is located at the C-terminal end of the N domain, and so is ideally placed to link movements of the N domain with changes in the transmembrane α-helices. The P2 helix is immediately N-terminal of the conserved sequence $D^{601}PPR^{604}$. Arg-604 is hydrogen bonded to Gly-354 in the phosphorylation loop and to Asp-737 at the top of the long transmembrane α-helix M5. However, P1 and P2 themselves form few hydrogen bonds and no salt bridges with the rest of the ATPase, suggesting that movement of P1 and P2 would not involve any large activation energy. Similarly, the M6–M7 loop should be able to move relative to the P domain, because there are no salt bridges and few hydrogen bonds linking the loop to the P domain.

Cys-344 is in a very interesting part of the structure, as described above. Cys-344 is labelled with high specificity by (4-bromomethyl)-6,7-dimethoxycoumarin. Labelling results in only a 30% decrease in ATPase activity [98], suggesting that, despite its critical position, the residue is not involved in any specific chemical interactions; consistent with this interpretation, Cys-344 is not conserved in the Ca^{2+}-ATPases. The labelled residue shows a very conformationally sensitive fluorescence, with phosphorylation with ATP or P_i leading to changes in fluorescence intensity [98]. Fluorescence also changes on addition of Mg^{2+} in a pH- and Ca^{2+}-sensitive manner; it was suggested that effects of pH and Mg^{2+} followed from binding at the gating site that controls access of Ca^{2+} to the high-affinity sites [25].

Other regions of the ATPase important in transport have been identified using mutagenesis. Mutants defective in transport have been classified depending on the response of the phosphorylated ATPase to the addition of ADP. The phosphorylated ATPase can exist in an ADP-sensitive form, where the rate of dephosphorylation is increased by addition of ADP because of the back-reaction of the phosphorylated ATPase with ADP forming ATP. Alternatively, the phosphorylated ATPase can be in an ADP-insensitive form, where addition of ADP does not affect the rate of dephosphorylation. In terms of Scheme 1, ADP-sensitive and -insensitive forms correspond to $E2PCa_2$ and E2P respectively. However, mutants that are trapped in the ADP-sensitive form are often referred to in the literature as E1P mutants [45]. The notation E1P was based on a reaction scheme for the ATPase in which an intermediate phosphorylated form, $E1PCa_2$, was proposed to form before $E2PCa_2$, although, as described above, results from kinetic experiments do not require such an intermediate [29].

There are a number of ways in which the phosphorylated ATPase could be locked in the ADP-sensitive form. One is that dissociation of Ca^{2+} from $E2PCa_2$ is blocked, so that the ADP-insensitive E2P is not formed from the ADP-sensitive $E2PCa_2$. Alternatively, mutation could block the phosphorylated ATPase in some intermediate state before formation of the normal $E2PCa_2$. A range of mutations have been found to block the ATPase in the phosphorylated, ADP-sensitive form [45]. Many are located in rather non-obvious regions of the structure and presumably have their effects through non-specific changes in conformation of the ATPase. For example, mutation of Thr-181, Gly-182 and Glu-183 in the A domain results in block in an ADP-sensitive form [45], and mutation of Arg-198 has been shown to reduce the rate of dephosphorylation [99]. However, a number of sensitive residues have been identified in the S4 stalk region and in the sequence connecting S4 to the P1 helix. For example, mutation of Pro-312 at the top of M4 gave an enzyme that was phosphorylated normally but was blocked in the $E2PCa_2$ form, so that the phosphorylated ATPase remained ADP-sensitive and the rate of dephosphorylation was very low; in contrast, phosphoenzyme formed from P_i in the absence of Ca^{2+} was dephosphorylated at the normal rate [100]. More detailed studies show that effects can be rather complex. For example, mutation of Leu-319 to Arg decreases the rate of phosphorylation when enzyme in the absence of Ca^{2+} is mixed with Ca^{2+} and ATP,

whereas there is little effect when ATPase in the presence of Ca^{2+} is mixed with ATP [101]. Thus a step leading to $E1'Ca_2$ is slowed. Mutation of residues in the S5 stalk region have also been shown to affect the rates of Ca^{2+} binding and of dephosphorylation [102]. These studies confirm the importance of the stalk region in the transport process.

Mutation of Lys-297 at the bottom of M4 on the lumenal side of the membrane also gave a mutant blocked in the ADP-sensitive, phosphorylated form [45]. Lys-297 forms a salt bridge with Glu-90 on the lumenal side, linking transmembrane α-helices M2 and M4 (Figure 9); it was argued above that the site of Ca^{2+} release into the lumen could be close to the M1–M2 lumenal loop. Some of the mutations in M4, M5 and M6 that reduce Ca^{2+} sensitivity also reduce the rate of dephosphorylation of E2P produced by phosphorylation with P_i [45]. This serves to demonstrate the link between the Ca^{2+} binding sites and the phosphorylation site, but the mechanism of the link is not clear. It is known that transport of Ca^{2+} by the ATPase is linked to movement of H^+ out of vesicles. It has been suggested that protonation of the residues at the empty Ca^{2+} binding sites in E2P is necessary for normal dephosphorylation of E2P, and that mutations at the Ca^{2+} binding sites could affect this protonation [45].

CONTROL OF THE Ca^{2+}-ATPase

The activity of the Ca^{2+}-ATPase in cardiac muscle is controlled by interaction with phospholamban, a 52-residue protein found in the SR membrane [103]. Reconstitution studies and co-expression studies have shown that the activity of skeletal muscle Ca^{2+}-ATPase is also modulated by interaction with phospholamban [103–106]. Phospholamban contains a hydrophilic N-terminal domain and a hydrophobic C-terminal domain, which forms a transmembrane α-helix [107]. It is agreed that binding of phospholamban to the Ca^{2+}-ATPase results in a reduced apparent affinity of the ATPase for Ca^{2+}, which is clear in studies of the rate of hydrolysis of ATP or of Ca^{2+} uptake as a function of Ca^{2+} concentration [103]. Direct studies of Ca^{2+} binding, however, detect no effect of phospholamban on Ca^{2+} affinity [105,108], so that the effects on apparent affinity detected in kinetic studies must follow from effects on the rates of one or more of the steps involved in Ca^{2+} binding. More controversial are effects of phospholamban on the rate of hydrolysis of ATP by phospholamban. Some groups detect effects on V_{max} [105,106,109,110] and some do not (see [103]). It has been suggested that the transmembrane domain of phospholamban is responsible for effects on the apparent affinity for Ca^{2+}, whereas the cytoplasmic domain is responsible for effects on V_{max} [105,106,109].

Phospholamban has been shown to interact with residues in the region $K^{397}NDKPV^{402}$ of skeletal muscle Ca^{2+}-ATPase [104]. These are located on the underside of the N domain (Figure 8) in a region shown in antibody binding experiments to be exposed [111]. This region stretches from 29 to 40 Å above the bilayer surface. The cytoplasmic domain of phospholamban contains about 30 residues, and so is able to reach up to this region of the ATPase. It has been suggested that the transmembrane region of phospholamban interacts with residues at the top of transmembrane α-helix M6 [112]; of the identified residues, Leu-802 and Thr-805 are on the outer face of M6, where they could interact with phospholamban (Figure 8).

The Ca^{2+}-ATPase is inhibited by a variety of hydrophobic molecules, including sesquiterpene lactones such as thapsigargin and trilobolide and simple hydroxy-containing molecules such as dihydroxybenzene [113–117]. The presence of hydroxy groups has been shown to be important in both sets of inhibitors [118]. The mechanism of inhibition is complex, involving more than the formation of a simple dead-end complex; a modified E2 conformation of the ATPase is produced, which is unable to undergo phosphorylation with P_i [114,116].

The S3 stalk region between residues 254 and 259 is important for binding thapsigargin and a third class of inhibitor, cyclopiazonic acid [119]. However, the effects of binding of the two inhibitors are distinct, since mutation of Phe-256 reduces the affinity for thapsigargin but not for cyclopiazonic acid [119]. The effect of Phe-256 on binding of thapsigargin is particularly important, since spontaneous mutations of Phe-256 were found in three cell lines following the development of resistance to thapsigargin [120]. The residues important in binding are located immediately above the interface, so that the hydroxy groups on the inhibitors presumably form hydrogen bonds with polar residues in the stalk region, with the hydrophobic groups on the inhibitors interacting with hydrophobic residues in the transmembrane α-helices.

CONCLUSIONS: ION PUMPS AND ION CHANNELS

Before the publication of the high-resolution structure of the Ca^{2+}-ATPase, there was much speculation that ion channels and ion pumps might be structurally rather similar. This is clearly not the case. Whereas with porins and ion channels such as the potassium channel KcsA the pathway for transport across the membrane is very obvious [56,57], this is not so for the Ca^{2+}-ATPase. Transport of the two bound Ca^{2+} ions across the membrane must involve a significant change in the packing of the transmembrane α-helices. It is this requirement for a significant conformational change that results in a rate of ion movement for the Ca^{2+}-ATPase that is very much lower than the rate of ion movement through an ion channel.

We thank the BBSRC and the Wellcome Trust for financial support. We also thank Dr Michael Green for many helpful discussions about the mechanism and structure of the calcium pump and for comments on a first draft of this review.

REFERENCES

1 Fagan, M. J. and Saier, M. H. (1994) P-type ATPases of eukaryotes and bacteria – sequence analyses and construction of phylogenetic trees. J. Mol. Evol. **38**, 57–99
2 Moller, J. V., Juul, B. and le Maire, M. (1996) Structural organization, ion transport, and energy transduction of P-type ATPases. Biochim. Biophys. Acta **1286**, 1–51
3 Toyoshima, C., Nakasako, M. and Ogawa, H. (2000) Crystal structure of the calcium pump of sarcoplasmic reticulum at 2.6 Å resolution. Nature (London) **405**, 647–655
4 MacLennan, D. H., Brandl, C. J., Korczak, B. and Green, N. M. (1985) Amino-acid sequence of a $Ca^{2+} + Mg^{2+}$-dependent ATPase from rabbit muscle sarcoplasmic reticulum, deduced from its complementary DNA sequence. Nature (London) **316**, 696–700
5 Aravind, L., Galperin, M. Y. and Koonin, E. V. (1998) The catalytic domain of the P-type ATPase has the haloacid dehalogenase fold. Trends Biochem. Sci. **23**, 127–129
6 Stokes, D. L. and Green, N. M. (2000) Modeling a dehalogenase fold into the 8-Å density map for Ca^{2+}-ATPase defines a new domain structure. Biophys. J. **78**, 1765–1776
7 Hisano, T., Hata, Y., Fujii, T., Liu, J. Q., Kurihara, T., Esaki, N. and Soda, K. (1996) Crystal structure of L-2-haloacid dehalogenase from *Pseudomonas* sp. YL. J. Biol. Chem. **271**, 20322–20330
8 Matthews, I., Colyer, J., Mata, A. M., Green, N. M., Sharma, R. P., Lee, A. G. and East, J. M. (1989) Evidence for the cytoplasmic location of the N- and C-terminal segments of sarcoplasmic reticulum (Ca^{2+}-Mg^{2+})-ATPase. Biochem. Biophys. Res. Commun. **161**, 683–688
9 Matthews, I., Sharma, R. P., Lee, A. G. and East, J. M. (1990) Transmembranous organisation of (Ca^{2+}-Mg^{2+})-ATPase from sarcoplasmic reticulum: evidence for the luminal location of residues 877–888. J. Biol. Chem. **265**, 18737–18740
10 Clarke, D. M., Loo, T. W. and MacLennan, D. H. (1990) The epitope for monoclonal antibody A20 (amino acids 870–890) is located on the luminal surface of the Ca^{2+}-ATPase of sarcoplasmic reticulum. J. Biol. Chem. **265**, 17405–17408

11 Champeil, P., Menguy, T., Soulie, S., Juul, B., de Gracia, A. G., Rusconi, F., Falson, P., Denoroy, L., Henao, F., le Maire, M. and Moller, J. V. (1998) Characterization of a protease-resistant domain of the cytosolic portion of sarcoplasmic reticulum Ca^{2+}-ATPase: nucleotide and metal-binding sites. J. Biol. Chem. **273**, 6619–6631

12 Andersen, J. P., Vilsen, B., Collins, J. H. and Jorgensen, P. L. (1986) Localization of E1-E2 conformational transitions of sarcoplasmic reticulum Ca-ATPase by tryptic cleavage and hydrophobic labeling. J. Membr. Biol. **93**, 85–92

13 Daiho, T., Yamasaki, K., Suzuki, H., Saino, T. and Kanazawa, T. (1999) Deletions or specific substitutions of a few residues in the NH_2-terminal region (Ala^3 to Thr^9) of sarcoplasmic reticulum Ca^{2+}-ATPase cause inactivation and rapid degradation of the enzyme expressed in COS-1 cells. J. Biol. Chem. **274**, 23910–23915

14 McPhalen, C. A., Strynadka, N. C. J. and James, M. N. G. (1991) Calcium-binding sites in proteins: a structural perspective. Adv. Protein Chem. **42**, 77–144

15 White, S. H. and Wimley, W. C. (1999) Membrane protein folding and stability: Physical principles. Annu. Rev. Biophys. Biomol. Struct. **28**, 319–365

16 de Meis, L. (1981) The Sarcoplasmic Reticulum, Wiley, New York

17 Suko, J., Plank, B., Preis, P., Kolassa, N., Hellmann, G. and Conca, W. (1981) Formation of magnesium-phosphoenzyme and magnesium-calcium-phosphoenzyme in the phosphorylation of adenosine triphosphatase by orthophosphate in sarcoplasmic reticulum. Models of a reaction sequence. Eur. J. Biochem. **119**, 225–236

18 Lacapere, J. J., Gingold, M. P., Champeil, P. and Guillain, F. (1981) Sarcoplasmic reticulum ATPase phosphorylation from inorganic phosphate in the absence of a calcium gradient. Steady state and kinetic fluorescence studies. J. Biol. Chem. **256**, 2302–2306

19 Martin, D. W. and Tanford, C. (1981) Phosphorylation of calcium adenosine triphosphatase by inorganic phosphate: van't Hoff analysis of enthalpy changes. Biochemistry **20**, 4597–4602

20 Jencks, W. P., Yang, T., Peisach, D. and Myung, J. (1993) Calcium ATPase of sarcoplasmic reticulum has 4 binding sites for calcium. Biochemistry **32**, 7030–7034

21 Khan, Y. M., East, J. M. and Lee, A. G. (1997) Effects of pH on phosphorylation of the Ca^{2+}-ATPase of sarcoplasmic reticulum by inorganic phosphate. Biochem. J. **321**, 671–676

22 Jencks, W. P. (1989) How does a calcium pump pump calcium? J. Biol. Chem. **264**, 18855–18858

23 Stahl, N. and Jencks, W. P. (1987) Reactions of the sarcoplasmic reticulum calcium adenosine triphosphatase with adenosine 5′-triphosphate and Ca^{2+} that are not satisfactorily described by an E1-E2 model. Biochemistry **26**, 7654–7667

24 Petithory, J. R. and Jencks, W. P. (1988) Binding of Ca^{2+} to the calcium adenosine triphosphatase of sarcoplasmic reticulum. Biochemistry **27**, 8626–8635

25 Henderson, I. M. J., Khan, Y. M., East, J. M. and Lee, A. G. (1994) Binding of calcium to the (Ca^{2+}-Mg^{2+})-ATPase of sarcoplasmic reticulum: Equilibrium studies. Biochem. J. **297**, 615–624

26 Dupont, Y. (1976) Fluorescence studies of the sarcoplasmic reticulum calcium pump. Biochem. Biophys. Res. Commun. **71**, 544–550

27 Reinstein, J. and Jencks, W. P. (1993) The binding of ATP and Mg^{2+} to the calcium adenosine triphosphatase of sarcoplasmic reticulum follows a random mechanism. Biochemistry **32**, 6632–6642

28 Petithory, J. R. and Jencks, W. P. (1986) Phosphorylation of the calcium adenosine triphosphatase of sarcoplasmic reticulum: Rate-limiting conformational change followed by rapid phosphoryl transfer. Biochemistry **25**, 4493–4497

29 Pickart, C. M. and Jencks, W. P. (1982) Slow dissociation of ATP from the calcium ATPase. J. Biol. Chem. **257**, 5319–5322

30 Pickart, C. M. and Jencks, W. P. (1984) Energetics of the calcium-transporting ATPase. J. Biol. Chem. **259**, 1629–1643

31 Gerstein, J. and Jencks, W. P. (1964) Equilibria and rates for acetyl transfer among substituted phenyl acetates, acetylimidazole, O-acetylhydroxamic acids, and thiol esters. J. Am. Chem. Soc. **86**, 4655–4663

32 Gould, G. W., East, J. M., Froud, R. J., McWhirter, J. M., Stefanova, H. I. and Lee, A. G. (1986) A kinetic model for the $Ca^{2+} + Mg^{2+}$-activated ATPase of sarcoplasmic reticulum. Biochem. J. **237**, 217–227

33 Champeil, P., Riollet, S., Orlowski, S., Guillain, F., Seebregts, C. J. and McIntosh, D. B. (1988) ATP regulation of sarcoplasmic reticulum Ca^{2+}-ATPase. Metal-free ATP and 8-bromo-ATP bind with high affinity to the catalytic site of phosphorylated ATPase and accelerate dephosphorylation. J. Biol. Chem. **263**, 12288–12294

34 Andersen, J. P. and Moller, J. V. (1985) The role of Mg^{2+} and Ca^{2+} in the simultaneous binding of vanadate and ATP at the phosphorylation site of sarcoplasmic reticulum Ca^{2+}-ATPase. Biochim. Biophys. Acta **815**, 9–15

35 Dupont, Y. (1980) Occlusion of divalent cations in the phosphorylated calcium pump of sarcoplasmic reticulum. Eur. J. Biochem. **109**, 231–238

36 Garrahan, P. J., Rega, A. F. and Alonso, G. L. (1976) The interaction of magnesium ions with the calcium pump of sarcoplasmic reticulum. Biochim. Biophys. Acta **448**, 121–132

37 Ogurusu, T., Wakabayashi, S. and Shigekawa, M. (1991) Activation of sarcoplasmic reticulum Ca^{2+}-ATPase by Mn^{2+}: A Mn^{2+} binding study. J. Biochem. (Tokyo) **109**, 472–476

38 Hill, T. L. and Inesi, G. (1982) Equilibrium cooperative binding of calcium and protons by sarcoplasmic reticulum ATPase. Proc. Natl. Acad. Sci. U.S.A. **79**, 3978–3982

39 Ogawa, J., Stokes, D. L., Sasabe, H. and Toyoshima, C. (1998) Structure of the Ca^{2+} pump of sarcoplasmic reticulum: a view along the lipid bilayer at 9-Å resolution. Biophys. J. **75**, 41–52

40 Stokes, D. L. and Lacapere, J. J. (1994) Conformation of Ca^{2+}-ATPase in two crystal forms. J. Biol. Chem. **269**, 11606–11613

41 Champeil, P., le Maire, M., Andersen, J. P., Guillain, F., Gingold, M., Lund, S. and Moller, J. V. (1986) Kinetic characterization of the normal and detergent-perturbed reaction cycles of the sarcoplasmic reticulum calcium pump. Rate-limiting step(s) under different conditions. J. Biol. Chem. **261**, 16372–16384

42 Silva, J. L. and Verjovski-Almeida, S. (1983) Self-association and modification of calcium binding in solubilized sarcoplasmic reticulum adenosine triphosphatase. Biochemistry **22**, 707–716

43 Froud, R. J. and Lee, A. G. (1986) Conformational transitions in the $Ca^{2+} + Mg^{2+}$-activated ATPase and the binding of Ca^{2+} ions. Biochem. J. **237**, 197–206

44 Clarke, D. M., Loo, T. W., Inesi, G. and MacLennan, D. H. (1989) Location of high affinity Ca^{2+}-binding sites within the predicted transmembrane domain of the sarcoplasmic reticulum Ca^{2+}-ATPase. Nature (London) **339**, 476–478

45 Andersen, J. P. (1995) Dissection of the functional domains of the sarcoplasmic reticulum Ca^{2+}-ATPase by site-directed mutagenesis. Biosci. Rep. **15**, 243–261

46 Fujimori, T. and Jencks, W. P. (1992) Binding of 2 Sr^{2+} ions changes the chemical specificities for phosphorylation of the sarcoplasmic-reticulum calcium ATPase through a stepwise mechanism. J. Biol. Chem. **267**, 18475–18487

47 Skerjanc, I. S., Toyofuku, T., Richardson, C. and MacLennan, D. H. (1993) Mutation of glutamate-309 to glutamine alters one Ca^{2+} binding site in the Ca^{2+}-ATPase of sarcoplasmic reticulum expressed in sf9 cells. J. Biol. Chem. **268**, 15944–15950

48 Zhang, Z. S., Lewis, D., Strock, C. and Inesi, G. (2000) Detailed characterization of the cooperative mechanism of Ca^{2+} binding and catalytic activation in the Ca^{2+} transport (SERCA) ATPase. Biochemistry **39**, 8758–8767

49 Andersen, J. P. and Vilsen, B. (1992) Functional consequences of alterations to Glu-309, Glu-771 and Asp-800 in the Ca-ATPase of sarcoplasmic reticulum. J. Biol. Chem. **267**, 19383–19387

50 Andersen, J. P. and Vilsen, B. (1994) Amino acids Asn^{796} and Thr^{799} of the Ca^{2+}-ATPase of sarcoplasmic reticulum bind Ca^{2+} at different sites. J. Biol. Chem. **269**, 15931–15936

51 Vilsen, B. and Andersen, J. P. (1992) CrATP-induced Ca^{2+} occlusion in mutants of the Ca^{2+}-ATPase of sarcoplasmic reticulum. J. Biol. Chem. **267**, 25739–25743

52 Lee, A. G. (1996) Structure of the SR/ER Ca^{2+}-ATPase. In Biomembranes, volume 5: The ATPases (Lee, A. G., ed.), pp. 1–42, JAI Press, Greenwich, CT

53 Vilsen, B. and Andersen, J. P. (1998) Mutation to the glutamate in the fourth membrane segment of Na^+,K^+-ATPase and Ca^{2+}-ATPase affects cation binding from both sides of the membrane and destabilizes the occluded enzyme forms. Biochemistry **37**, 10961–10971

54 Rice, W. J. and MacLennan, D. H. (1996) Scanning mutagenesis reveals a similar pattern of mutation sensitivity in transmembrane sequences M4, M5, and M6, but not in M8, of the Ca^{2+}-ATPase of sarcoplasmic reticulum (SERCA1a). J. Biol. Chem. **271**, 31412–31419

55 Andersen, J. P. (1995) Functional consequences of alterations to amino acids at the M5S5 boundary of the Ca^{2+}-ATPase of sarcoplasmic reticulum. J. Biol. Chem. **270**, 908–914

56 Cowan, S. W. (1993) Bacterial porins: lessons from three high-resolution structures. Curr. Opin. Struct. Biol. **3**, 501–507

57 Doyle, D. A., Cabral, J. M., Pfuetzner, R. A., Kuo, A., Gulbis, J. M., Cohen, S. L., Chait, B. T. and Mackinnon, R. (1998) The structure of the potassium channel: molecular basis of K^+ conduction and selectivity. Science **280**, 69–77

58 Menguy, T., Corre, F., Bouneau, L., Deschamps, S., Moller, J. V., Champeil, P., le Maire, M. and Falson, P. (1998) The cytoplasmic loop located between transmembrane segments 6 and 7 controls activation by Ca^{2+} of sarcoplasmic reticulum Ca^{2+}-ATPase. J. Biol. Chem. **273**, 20134–20143

59 Dupont, Y. (1982) Low-temperature studies of the sarcoplasmic reticulum calcium pump. Mechanisms of calcium binding. Biochim. Biophys. Acta **688**, 75–87

60 Inesi, G. (1987) Sequential mechanism of calcium binding and translocation in sarcoplasmic reticulum adenosine triphosphatase. J. Biol. Chem. **262**, 16338–16342

61 Orlowski, S. and Champeil, P. (1991) Kinetics of calcium dissociation from its high-affinity transport sites on sarcoplasmic reticulum ATPase. Biochemistry **30**, 352–361

62 Henderson, I. M. J., Starling, A. P., Wictome, M., East, J. M. and Lee, A. G. (1994) Binding of calcium to the (Ca^{2+}-Mg^{2+})-ATPase of sarcoplasmic reticulum: kinetic studies. Biochem. J. **297**, 625–636

63 Lee, A. G., Baker, K., Khan, Y. M. and East, J. M. (1995) Effects of K^+ on the binding of Ca^{2+} to the Ca^{2+}-ATPase of sarcoplasmic reticulum. Biochem. J. **305**, 225–231

64 Moutin, M. J. and Dupont, Y. (1991) Interaction of potassium and magnesium with the high affinity calcium-binding sites of the sarcoplasmic reticulum calcium-ATPase. J. Biol. Chem. **266**, 5580–5586

65 Clarke, D. M., Maruyama, K., Loo, T. W., Leberer, E., Inesi, G. and MacLennan, D. H. (1989) Functional consequences of glutamate, aspartate, glutamine, and asparagine mutations in the stalk sector of the Ca^{2+}-ATPase of sarcoplasmic reticulum. J. Biol. Chem. **264**, 11246–11251

66 Dupont, Y., Pougeois, R., Ronjat, M. and Verjovsky-Almeida, S. (1985) Two distinct classes of nucleotide binding sites in sarcoplasmic reticulum Ca-ATPase revealed by 2′,3′-O-(2,4,6-trinitrocyclohexadienylidene)-ATP. J. Biol. Chem. **260**, 7241–7249

67 Yonekura, K., Stokes, D. L., Sasabe, H. and Toyoshima, C. (1997) The ATP-binding site of Ca^{2+}-ATPase revealed by electron image analysis. Biophys. J. **72**, 997–1005

68 Stokes, D. L. and Wagenknecht, T. (2000) Calcium transport across the sarcoplasmic reticulum – Structure and function of Ca^{2+}-ATPase and the ryanodine receptor. Eur. J. Biochem. **267**, 5274–5279

69 Baker, K. J., East, J. M. and Lee, A. G. (1994) Localization of the hinge region of the Ca^{2+}-ATPase of sarcoplasmic reticulum using resonance energy transfer. Biochim. Biophys. Acta **1192**, 53–60

70 Gutierrez-Merino, C., Munkonge, F., Mata, A. M., East, J. M., Levinson, B. L., Napier, R. M. and Lee, A. G. (1987) The position of the ATP binding site on the (Ca^{2+}-Mg^{2+})-ATPase. Biochim. Biophys. Acta **897**, 207–216

71 Birck, C., Mourey, L., Gouet, P., Fabry, B., Schumacher, J., Rousseau, P., Kahn, D. and Samama, J. P. (1999) Conformational changes induced by phosphorylation of the FixJ receiver domain. Structure **7**, 1505–1515

72 Maruyama, K., Clarke, D. M., Fujii, J., Inesi, G., Loo, T. W. and MacLennan, D. H. (1989) Functional consequences of alterations to amino acids located in the catalytic center (isoleucine 348 to threonine 357) and nucleotide-binding domain of the Ca^{2+}-ATPase of sarcoplasmic reticulum. J. Biol. Chem. **264**, 13038–13042

73 McIntosh, D. B., Woolley, D. G., MacLennan, D. H., Vilsen, B. and Andersen, J. P. (1999) Interaction of nucleotides with Asp^{351} and the conserved phosphorylation loop of sarcoplasmic reticulum Ca^{2+}-ATPase. J. Biol. Chem. **274**, 25227–25236

74 Lacapere, J. J. and Guillain, F. (1993) The reaction-mechanism of Ca^{2+}-ATPase of sarcoplasmic-reticulum – direct measurement of the Mg.ATP dissociation-constant gives similar values in the presence or absence of calcium. Eur. J. Biochem. **211**, 117–126

75 Mitchinson, C., Wilderspin, A. F., Trinnaman, B. J. and Green, N. M. (1982) Identification of a labelled peptide after stoichiometric reaction of fluorescein isothiocyanate with the Ca^{2+}-dependent adenosine triphosphatase of sarcoplasmic reticulum. FEBS Lett. **146**, 87–92

76 Yamamoto, H., Tagaya, M., Fukui, T. and Kawakita, M. (1988) Affinity labeling of the ATP-binding site of Ca^{2+}-transporting ATPase of sarcoplasmic reticulum by adenosine triphosphopyridoxal: identification of the reactive lysyl residue. J. Biochem. (Tokyo) **103**, 452–457

77 Yamamoto, H., Imamura, Y., Tagaya, M., Fukui, T. and Kawakita, M. (1989) Ca^{2+}-dependent conformational change of the ATP-binding site of Ca^{2+}-transporting ATPase of sarcoplasmic reticulum as revealed by an alteration of the target-site specificity of adenosine triphosphopyridoxal. J. Biochem. (Tokyo) **106**, 1121–1125

78 McIntosh, D. B. (1992) Glutaraldehyde cross-links Lys-492 and Arg-678 at the active site of sarcoplasmic reticulum Ca^{2+}-ATPase. J. Biol. Chem. **267**, 22328–22335

79 McIntosh, D. B., Ross, D. C., Champeil, P. and Guillain, F. (1991) Crosslinking the active site of sarcoplasmic reticulum Ca^{2+}-ATPase completely blocks Ca^{2+} release to the vesicle lumen. Proc. Natl. Acad. Sci. U.S.A. **88**, 6437–6441

80 McIntosh, D. B. and Woolley, D. G. (1994) Catalysis of an ATP analogue untethered and tethered to lysine 492 of sarcoplasmic reticulum Ca^{2+}-ATPase. J. Biol. Chem. **269**, 21587–21595

81 Froud, R. J., Earl, C. R. A., East, J. M. and Lee, A. G. (1986) Effects of lipid fatty acyl chain structure on the activity of the ($Ca^{2+} + Mg^{2+}$)-ATPase. Biochim. Biophys. Acta **860**, 354–360

82 Starling, A. P., Khan, Y. M., East, J. M. and Lee, A. G. (1994) Characterization of the single Ca^{2+} binding site on the Ca^{2+}-ATPase reconstituted with short and long chain phosphatidylcholines. Biochem. J. **304**, 569–575

83 Deisenhofer, J., Epp, O., Miki, K., Huber, R. and Michel, H. (1985) Structure of the protein subunits in the photosynthetic reaction center of *Rhodopseudomonas viridis* at 3 Å resolution. Nature (London) **318**, 618–624

84 McDermott, G., Prince, S. M., Freer, A. A., Hawthornthwaite-Lawless, A. M., Papiz, M. Z., Cogdell, R. J. and Isaacs, N. W. (1995) Crystal structure of an integral membrane light-harvesting complex from photosynthetic bacteria. Nature (London) **374**, 517–521

85 Zhang, Z., Huang, L., Shulmeister, V. M., Chi, Y. I., Kim, K. K., Hung, L. W., Crofts, A. R., Berry, E. A. and Kim, S. H. (1998) Electron transfer by domain movement in cytochrome bc_1. Nature (London) **392**, 677–684

86 Tsukihara, T., Aoyama, H., Yamashita, E., Tomizaki, T., Yamaguchi, H., Shinzawa-Itoh, K., Nakashima, R., Yaono, R. and Yoshikawa, S. (1996) The whole structure of the 13-subunit oxidized cytochrome c oxidase at 2.8 Å. Science **272**, 1136–1144

87 Iverson, T. M., Luna-Chavez, C., Cecchini, G. and Rees, D. C. (1999) Structure of the *Escherichia coli* fumarate reductase respiratory complex. Science **284**, 1961–1966

88 Chang, G., Spencer, R. H., Lee, A. T., Barclay, M. T. and Rees, D. C. (1998) Structure of the MscL homolog from Mycobacterium tuberculosis: A gated mechanosensitive ion channel. Science **282**, 2220–2226

89 Lewis, B. A. and Engelman, D. M. (1983) Lipid bilayer thickness varies linearly with acyl chain length in fluid phosphatidylcholine vesicles. J. Mol. Biol. **166**, 211–217

90 Sperotto, M. M. and Mouritsen, O. G. (1988) Dependence of lipid membrane phase transition temperature on the mismatch of protein and lipid hydrophobic thickness. Eur. Biophys. J. **16**, 1–10

91 Webb, R. J., Khan, Y. M., East, J. M. and Lee, A. G. (2000) The importance of carboxyl groups on the lumenal side of the membrane for the function of the Ca^{2+}-ATPase of sarcoplasmic reticulum. J. Biol. Chem. **275**, 977–982

92 Orlowski, S. and Champeil, P. (1991) The two calcium ions initially bound to nonphosphorylated sarcoplasmic reticulum Ca-ATPase can no longer be kinetically distinguished when they dissociate from phosphorylated ATPase toward the lumen. Biochemistry **30**, 11331–11342

93 Hanel, A. M. and Jencks, W. P. (1991) Dissociation of calcium from the phosphorylated calcium-transporting adenosine triphosphatase of sarcoplasmic reticulum: kinetic equivalence of the calcium ions bound to the phosphorylated enzyme. Biochemistry **30**, 11320–11330

94 Duggleby, R. C., East, J. M. and Lee, A. G. (1999) Luminal dissociation of Ca^{2+} from the phosphorylated Ca^{2+}-ATPase is sequential and gated by Mg^{2+}. Biochem. J. **339**, 351–357

95 Forge, V., Mintz, E., Canet, D. and Guillain, F. (1995) Lumenal Ca^{2+} dissociation from the phosphorylated Ca^{2+}-ATPase of the sarcoplasmic reticulum is sequential. J. Biol. Chem. **270**, 18271–18276

96 Myung, J. and Jencks, W. P. (1994) Lumenal and cytoplasmic binding sites for calcium on the calcium ATPase of sarcoplasmic reticulum are different and independent. Biochemistry **33**, 8775–8785

97 Falson, P., Menguy, T., Corre, F., Bouneau, L., Gomez de Gracia, A., Soulie, S., Centeno, F., Moller, J. V., Champeil, P. and le Maire, M. (1997) The cytoplasmic loop between putative transmembrane segments 6 and 7 in sarcoplasmic reticulum Ca^{2+}-ATPase binds Ca^{2+} and is functionally important. J. Biol. Chem. **272**, 17258–17262

98 Stefanova, H. I., East, J. M., Gore, M. G. and Lee, A. G. (1992) Labeling the (Ca^{2+}-Mg^{2+})-ATPase of sarcoplasmic reticulum with 4-bromomethyl-6,7-dimethoxycoumarin: detection of conformational changes. Biochemistry **31**, 6023–6031

99 Daiho, T., Suzuki, H., Yamasaki, K., Saino, T. and Kanazawa, T. (1999) Mutations of Arg^{198} in sarcoplasmic reticulum Ca^{2+}-ATPase cause inhibition of hydrolysis of the phosphoenzyme intermediate formed from inorganic phosphate. FEBS Lett. **444**, 54–58

100 Vilsen, B., Andersen, J. P., Clarke, D. M. and MacLennan, D. H. (1989) Functional consequences of proline mutations in the cytoplasmic and transmembrane sectors of the Ca^{2+}-ATPase of sarcoplasmic reticulum. J. Biol. Chem. **264**, 21024–21030

101 Sorensen, T. L. M., Dupont, Y., Vilsen, B. and Andersen, J. P. (2000) Fast kinetic analysis of conformational changes in mutants of the Ca^{2+}-ATPase of sarcoplasmic reticulum. J. Biol. Chem. **275**, 5400–5408

102 Sorensen, T. L. M. and Andersen, J. P. (2000) Importance of stalk segment S5 for intramolecular communication in the sarcoplasmic reticulum Ca^{2+}-ATPase. J. Biol. Chem. **275**, 28954–28961

103 Simmerman, H. K. B. and Jones, L. R. (1998) Phospholamban: protein structure, mechanism of action, and role in cardiac function. Physiol. Rev. **78**, 921–947

104 Toyofuku, T., Kurzydlowski, K., Tada, M. and MacLennan, D. H. (1994) Amino acids Lys-Asp-Asp-Lys-Pro-Val-402 in the Ca^{2+}-ATPase of cardiac sarcoplasmic reticulum are critical for functional association with phospholamban. J. Biol. Chem. **269**, 22929–22932

105 Hughes, G., Starling, A. P., Sharma, R. P., East, J. M. and Lee, A. G. (1996) Mechanism of inhibition of the Ca^{2+}-ATPase of sarcoplasmic reticulum by phospholamban. Biochem. J. **318**, 973–979

106 Sasaki, T., Inui, M., Kimura, Y., Kuzuya, T. and Tada, M. (1992) Molecular mechanism of regulation of Ca^{2+} pump ATPase by phospholamban in cardiac sarcoplasmic reticulum. Effects of synthetic phospholamban peptides on Ca^{2+} pump ATPase. J. Biol. Chem. **267**, 1674–1679

107 Ahmed, Z., Reid, D. G., Watts, A. and Middleton, D. A. (2000) A solid-state NMR study of the phospholamban transmembrane domain: local structure and interactions with Ca^{2+}-ATPase. Biochim. Biophys. Acta **1468**, 187–198

108 Cantilina, T., Sagara, Y., Inesi, G. and Jones, L. R. (1993) Comparative studies of cardiac and skeletal sarcoplasmic reticulum ATPases – effect of a phospholamban antibody on enzyme activation by Ca^{2+}. J. Biol. Chem. **268**, 17018–17025

109 Hughes, G., East, J. M. and Lee, A. G. (1994) The hydrophilic domain of phospholamban inhibits the Ca^{2+}-ATPase transport step of the Ca^{2+}-ATPase. Biochem. J. **303**, 511–516

110 Kargacin, M. E., Ali, Z. and Kargacin, G. J. (1998) Anti-phospholamban and protein kinase A alter the Ca^{2+} sensitivity and maximum velocity of Ca^{2+} uptake by the cardiac sarcoplasmic reticulum. Biochem. J. **331**, 245–249

111 Mata, A. M., Matthews, I., Tunwell, R. E. A., Sharma, R. P., Lee, A. G. and East, J. M. (1992) Definition of surface exposed and trans-membranous regions of the (Ca^{2+}-Mg^{2+})-ATPase of sarcoplasmic reticulum using anti-peptide antibodies. Biochem. J. **286**, 567–580

112 Asahi, M., Kimura, Y., Kurzydlowski, R., Tada, M. and MacLennan, D. H. (1999) Transmembrane helix M6 in sarco(endo)plasmic reticulum Ca^{2+}-ATPase forms a functional interaction site with phospholamban – evidence for physical interactions at other sites. J. Biol. Chem. **274**, 32855–32862

113 Thastrup, O., Cullen, P. J., Drbak, B. K., Hanley, M. R. and Dawson, A. P. (1990) Thapsigargin, a tumor promoter, discharges intracellular Ca^{2+} stores by specific inhibition of the endoplasmic reticulum Ca^{2+}-ATPase. Proc. Natl. Acad. Sci. U.S.A. **87**, 2466–2470

114 Wictome, M., Khan, Y. M., East, J. M. and Lee, A. G. (1995) Binding of sesquiterpene lactone inhibitors to the Ca^{2+}-ATPase. Biochem. J. **310**, 859–868

115 Llopis, J., Chow, S. B., Kass, G. E. N., Gahm, A. and Orrenius, S. (1991) Comparison between the effects of the microsomal Ca^{2+}-translocase inhibitors thapsigargin and 2,5-di-(tert-butyl)-1,4-benzohydroquinone on cellular calcium fluxes. Biochem. J. **277**, 553–556

116 Khan, Y. M., Wictome, M., East, J. M. and Lee, A. G. (1995) Interactions of dihydroxybenzenes with the Ca^{2+}-ATPase: separate binding sites for dihydroxybenzenes and sesquiterpene lactones. Biochemistry **34**, 14385–14393

117 Wictome, M., Starling, A. P., Sharma, R. P., East, J. M. and Lee, A. G. (1993) Inhibition of the Ca^{2+}-ATPase by sesquiterpene lactones. Biochem. Soc. Trans. **21**, 348S

118 Wictome, M., Holub, M., East, J. M. and Lee, A. G. (1994) The importance of the hydroxyl moieties for inhibition of the Ca^{2+}-ATPase by trilobolide and 2,5-di(ter-butyl)-1,4-benzohydroquinone. Biochem. Biophys. Res. Commun. **199**, 916–921

119 Ma, H., Zhong, L., Inesi, G., Fortea, I., Soler, F. and Fernandez-Belda, F. (1999) Overlapping effects of S3 stalk segment mutations on the affinity of Ca^{2+}-ATPase (SERCA) for thapsigargin and cyclopiazonic acid. Biochemistry **38**, 15522–15527

120 Yu, M., Lin, J., Khadeer, M., Yeh, Y., Inesi, G. and Hussain, A. (1999) Effects of various amino acid 256 mutations on sarcoplasmic/endoplasmic reticulum Ca^{2+}-ATPase function and their role in the cellular adaptive response to thapsigargin. Arch. Biochem. Biophys. **362**, 225–232

121 Brandl, C. J., Green, N. M., Korczak, B. and MacLennan, D. H. (1986) Two Ca^{2+} ATPase genes: homologies and mechanistic implications of deduced amino acid sequences. Cell **44**, 597–607

122 Lockyer, P. J., Puente, E., Windass, J., Earley, F., East, J. M. and Lee, A. G. (1998) Cloning and expression of an insect Ca^{2+}-ATPase from *Heliothis virescens*. Biochim. Biophys. Acta **1369**, 14–18

123 Palmero, I. and Sastre, L. (1989) Complementary DNA cloning of a protein highly homologous to mammalian sarcoplasmic reticulum Ca^{2+}-ATPase from the crustacean Artemia. J. Mol. Biol. **210**, 737–748

124 Wimmers, L. E., Ewing, N. N. and Bennett, A. B. (1992) Higher plant Ca^{2+}-ATPase – primary structure and regulation of messenger RNA abundance by salt. Proc. Natl. Acad. Sci. U.S.A. **89**, 9205–9209

125 Verma, A. K., Filoteo, A. G., Stanford, D. R., Wieben, E. D., Penniston, J. T., Strehler, E. E., Fischer, R., Heim, R., Vogel, G., Mathews, S. et al. (1988) Complete primary sequence of a human plasma membrane Ca^{2+} pump. J. Biol. Chem. **263**, 14152–14159